Composites: Part A 42 (2011) 2126–2142

Contents lists available at SciVerse ScienceDirect

Composites: Part A

journal homepage: www.elsevier.com/locate/compositesa

Review

Review of the mechanical properties of carbon nanofiber/polymer composites

Mohammed H. Al-Saleh [a,b,*], Uttandaraman Sundararaj [b,*]

[a] Department of Chemical Engineering, Jordan University of Science and Technology, P.O. Box 3030, Irbid 22110, Jordan
[b] Department of Chemical and Petroleum Engineering, Schulich School of Engineering, University of Calgary, 2500 University Drive N.W., Calgary, Alberta, Canada T2N 1N4

ARTICLE INFO

Article history:
Received 6 March 2011
Received in revised form 2 August 2011
Accepted 8 August 2011
Available online 16 September 2011

Keywords:
A. Carbon fiber
A. Polymer-matrix composites (PMCs)
B. Mechanical properties
B. Rheological properties

ABSTRACT

In this paper, the mechanical properties of vapor grown carbon nanofiber (VGCNF)/polymer composites are reviewed. The paper starts with the structural and intrinsic mechanical properties of VGCNFs. Then the major factors (filler dispersion and distribution, filler aspect ratio, adhesion and interface between filler and polymer matrix) affecting the mechanical properties of VGCNF/polymer composites are presented. After that, VGCNF/polymer composite mechanical properties are discussed in terms of nanofibers dispersion and alignment, adhesion between the nanofiber and polymer matrix, and other factors. The influence of processing methods and processing conditions on the properties of VGCNF/polymer composite is also considered. At the end, the possible future challenges for VGCNF and VGCNF/polymer composites are highlighted.

Contents

1. Introduction

Polymer composites are attractive for variety of applications due to many features including low weight, low cost, ease of processing and shaping, and corrosion resistance. Fillers are typically

* Corresponding authors. Address: Department of Chemical Engineering, Jordan University of Science and Technology, P.O. Box 3030, Irbid 22110, Jordan. Tel.: +962 2720100x22415; fax: +962 27201074 (M.H. Al-Saleh), tel.: +1 403 220 5750; fax: +1 403 284 4852 (U. Sundararaj).
E-mail addresses: mhsaleh@just.edu.jo (M.H. Al-Saleh), u.sundararaj@ucalgary.ca (U. Sundararaj).

1359-835X/$ - see front matter © 2011 Elsevier Ltd. All rights reserved.
doi:10.1016/j.compositesa.2011.08.005

Abbreviations

ABS	acrylonitrile–butadiene–styrene
CB	carbon black
CF	carbon fiber
CNT	carbon nanotubes
CNF	carbon nanofiber
DR	draw ratio
EFF	extrusion freeform fabrication
EMI	electromagnetic interference
ESD	electrostatic discharge
HDPE	high density polyethylene
HIPS	high impact polystyrene
HRTEM	high resolution transmission electron microscopy
VGCF	vapor grown carbon fiber
VGCNF	vapor grown carbon nanofibers
MNW	metal nanowire
MWCNT	Multi-walled carbon nanotubes
PE	polyethylene
PEEK	poly(ether ether ketone)
PES	poly(ether sulfone)
PET	poly(ethylene terephthalate)
PMMA	poly(methyl methacrylate)
PP	polypropylene
PS	Polystyrene
PVA	poly(vinyl alcohol)
PVDF	poly(vinylidene fluoride)
SEM	scanning electron microscope
s-VGCF	sub-micron-vapor grown carbon fiber
SWCNT	single wall carbon nanotube
T_g	glass transition temperature
TEM	transmission electron microscopy

added to enhance chemical and/or physical properties of polymers. Of these properties, optimizing the mechanical properties has been the most desired objective. Inorganic fibers (glass and carbon fibers) and aromatic organic fibers (Aramid) are the traditional fillers used to boost the mechanical properties of polymers. Since the reinforcing capabilities of fibers increases with decrease in their diameter [1], nanofibers have higher reinforcing capabilities than microfibers. With decreasing fiber diameter: the ultimate tensile strength of fiber increases due to a decrease in number of defects; the contact area between filler and polymer matrix increases due to an increase in fiber surface area/volume ratio; and the fiber flexibility increases. The increase in fiber flexibility allows the fiber to retain its aspect ratio because the fiber can bent without breaking and it is well known that higher aspect ratio leads to better mechanical properties. Moreover, polymers filled with nanofillers have better surface finish than those filled with microfiller because of the smaller size of filler [2].

Therefore, there is increasing interest to replace traditional microfiber/polymer composites with nanofiber/polymer composites. Thus, nanostructured polymeric materials based on carbon nanotubes (CNTs) and clay platelets, and to a lesser extent on vapor grown carbon nanofibers (VGCNFs), have been the subject of intense investigation [2–10]. When a material with multifunctional properties (mechanical, electrical, thermal, etc.) is required, carbon based nanostructured polymeric materials are favored over those based on the relatively cheaper and higher aspect ratio clay platelets. The mechanical properties of VGCNFs and their composites are the focus of this review. It is out of the scope of this paper to review mechanical properties of CNTs and their composites. However, we have summarized some of the most significant contributions attained using CNTs for purposes of comparison.

Even though VGCNFs were introduced few years before CNTs, they have received less research interest than CNTs. The major reasons are that single-wall carbon nanotubes (SWCNTs) and multi-walled carbon nanotubes (MWCNTs) produced by arc discharge and laser ablation have better mechanical properties than VGCNFs, and CNTs have smaller diameter and lower density than VGCNFs. However, because of their much lower price, VGCNFs are an excellent alternative for CNTs. VGCNFs could also be used for research purposes to build knowledge that might be transferable to more expensive CNTs, or used in combination with CNTs to create bi-filler composites with synergistic properties. Furthermore, the unique structure of the most common type of VGCNFs, which is the cup-stacked, contains more reactive carbon edges that can be functionalized to interact with the matrix, and thereby facilitate VGCNFs dispersion and enhance stress transfer from the polymer matrix to the nanofiller. VGCNFs are expected to be economically viable for many applications as a replacement for conventional carbon fibers (CFs) [7,11].

In addition to the applications that utilize VGCNFs as reinforcer, VGCNFs/polymer composite materials can be used in electromagnetic interference (EMI) shielding and electrostatic discharge (ESD) protection markets. A level of EMI shielding (~42 dB) can be obtained using a 2 mm plate made of a polymer composite containing 7.5 vol% VGCNF [12–14]. For ESD applications, because of the high aspect ratio of VGCNF, 0.5 vol% VGCNF was found enough to create a conductive network in an insulating polypropylene (PP) matrix [8]. It has also been reported that VGCNF/polymer composites can be used as sensors for organic vapors [15]. VGCNFs are promising materials for batteries, where multifunctional carbon materials are used as electrodes or as support materials [1]. For this application, carbon materials have many advantages over other materials such as metal oxides and sulfides in terms of cost, thermal and chemical stability, types of possible shapes and environmental impact [16]. VGCNFs have been investigated in the field of heterogeneous catalysis as a catalyst and/or catalyst support [17]. Polymers filled with VGCNFs have potential biological applications that require incorporation of biological components such

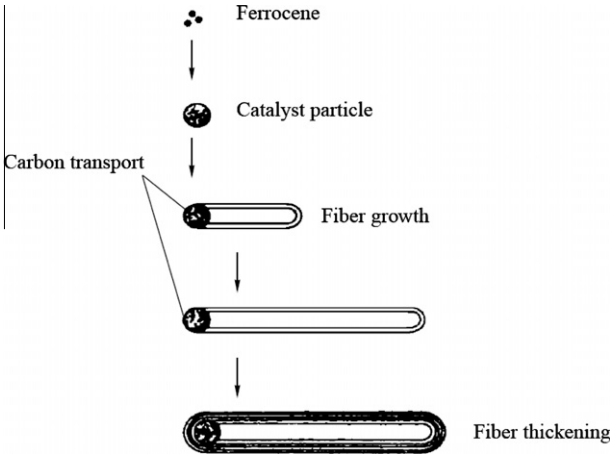

Fig. 1. Proposed mechanism for the growth in VGCNF diameter and length [7].

Table 1
Typical properties of VGCNF, SWCNT, MWCNT and CF.

Property	VGCNF[a]	SWCNT[b]	MWCNT[b]	CF[c]
Diameter (nm)	50–200	0.6–0.8	5–50	7300
Aspect ratio	250–2000	100–10,000	100–10,000	440
Density (g/cm^3)	2	~1.3[d]	~1.75[e]	1.74
Thermal conductivity (W/m K)	1950	3000–6000[f]	3000–6000[f]	20
Electrical resistivity (Ω cm)	1×10^{-4}	1×10^{-3}–1×10^{-4}	2×10^{-3}–1×10^{-4}	1.7×10^{-3}
Tensile strength (GPa)	2.92	50–500[g]	10–60[g]	3.8
Tensile modulus (GPa)	240	1500	1000	227

[a] From Refs. [3,8,22].
[b] From Ref. [5].
[c] Properties of Akzo nobel Fortafil 243 PAN-based fibers [23].
[d] From Ref. [24].
[e] From Ref. [25].
[f] From Ref. [26].
[g] From Ref. [27].

as proteins and DNAs in the hollow core of the fiber [18]. In addition to the above mentioned applications, VGCNFs could be used in many applications currently using conventional CFs and carbon black (CB).

2. VGCNF

VGCNFs are typically produced by pyrolysis of a hydrocarbon feedstock (natural gas, acetylene, etc.) or carbon monoxide on a metal catalyst such as iron. This process is considered the most promising technique for mass production of VGCNF of well defined diameter at relatively low cost [7,8]. The iron catalyst nanoparticles are produced by pyrolysis of organometallic compounds, such as ferrocene $Fe(C_5H_5)_2$ and iron pentacarbonyl $Fe(CO)_5$ [19]. The decomposition of the hydrocarbon grows the nanofibers. Fiber thickness depends on the catalyst size, operating conditions and catalyst activity [7]. In the reactor, growth in VGCNF thickness and length is not a simultaneous process, as illustrated in Fig. 1 [7]. Thickening of the fiber starts when the catalyst activity decreases and reaction temperature increases [7].

Properties of a VGCNF depends on its structure which in turn is a function of the production technique (feedstock, catalysts, etc.) and post-treatment methods [20]. In our previous review paper [13], we described in some detail the structure and the electrical and thermal properties of VGCNFs. In this work, we place emphasis on the mechanical properties and other related interesting features of the VGCNFs structure. Readers are advised to refer to our previous work and the work of Uchida and coworkers [21] for detailed information about VGCNF structures. Table 1 summaries some of the major properties of VGCNF, SWCNT, MWCNT and CF. Electrical resistivity of heat treated VGCNF is similar to that of CNTs, app. 1×10^{-4} Ω cm [13]. Thermal conductivity of VGCNF (1950 W/m K) is close to that of CNTs (~3000–6000 W/m K) and 2 orders of magnitude higher than conventional carbon fibers (CFs).

2.1. Dimensions and structure

VGCNFs have high aspect ratio. They have larger diameters than CNTs. Their typical diameter is in the range of 50–200 nm. The length of a VGCNF can be up to 100 μm. In our lab, we measured the length and diameter of Pyrograf III™ (PR-24-LHT) which is a low heat treated (LHT) carbon nanofiber produced by Applied Sciences, Inc., Ohio – USA. The dimensions of the (PR-24-LHT) VGCNF was characterized by analyzing scanning electron microscope (SEM) micrographs of well dispersed nanofibers on Isopore™ polycarbonate film membrane having an average pore diameter of 0.4 μm (Isopore™, Fisher Scientific) [28]. The well dispersed nanofibers on the Isopore™ membrane was prepared by first dispersing a small amount of the as-received LHT-VGCNF by sonication in methanol. The sonication was carried out for 20 s in a sonicator having an output power of 120 W, or for 1–2 min in a sonicator having an output power of 20 W. A few droplets of the sonicated VGCNF/methanol solution were then filtered on the Isopore membrane. It is very difficult to characterize the length of the as-grown VGCNF without sonication since as-received fibers are agglomerated and highly entangled as shown in Fig. 2.

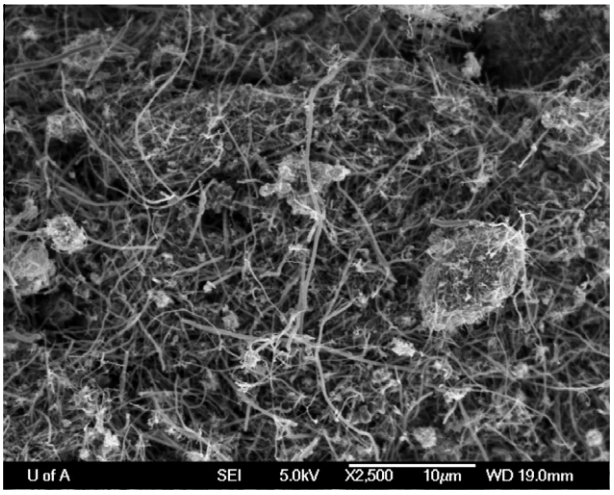

Fig. 2. SEM micrograph shows the agglomeration and entanglements of as-grown VGCNF.

The length of nanofibers is a crucial parameter that has a significant influence on the composites properties. We found that the (PR-24-LHT) VGCNF has a number average length and a diameter of 4.2 ± 4.0 μm and 110 ± 27 nm, respectively [28]. These numbers give nanofiber with an average aspect ratio of 38. Fig. 3 is a histogram showing the length distribution of (PR-24-LHT) VGCNF. It is apparent that the length of most nanofibers is in the range of 2–6 μm. Jimenez and Jana [29] found that almost 60% of Pyrograf III™ (PR-24-PS) after compounding with PMMA in a low shear Chaotic mixer have an average length between 2–6 μm. The PMMA matrix was removed by extraction and no sonication was used. Moreover, Uchida and coworkers [21] reported that the number and weight average length of Pyrograph III™ (PR-24-HT) are 2 μm and 8 μm, respectively.

VGCNFs are hollow core nanofibers consisting of a single graphite layer or double graphite layers that are stacked parallel or at a certain angle from the fiber axis [21,30]. The stacked layer are nested with each other and have different structures including

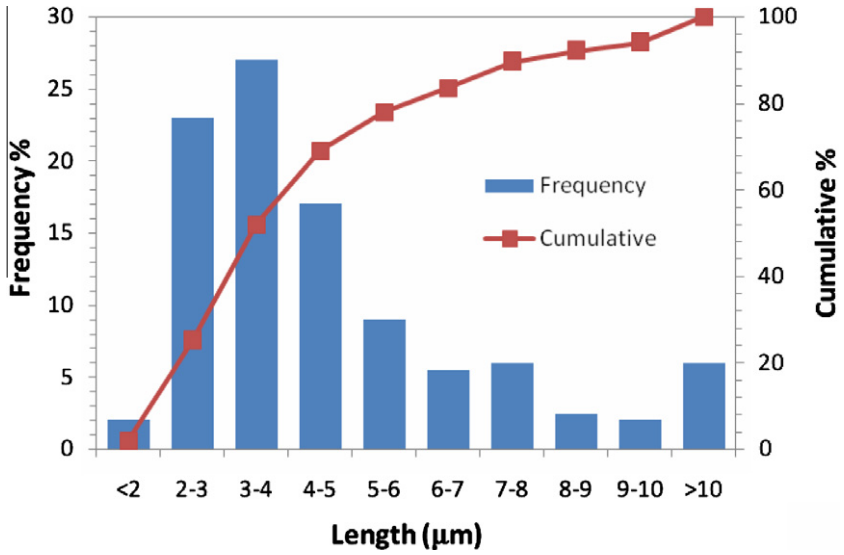

Fig. 3. Length distribution of Pyrograph III™ (PR-24-HT) VGCNF [28]. (For interpretation of the references to color in this figure legend, the reader is referred to the web version of this article.)

bamboo-like, parallel and cup-stacked [30–33]. Fig. 4 is a high resolution transmission electron microscopy (HRTEM) image of a side-wall of VGCNF (the inset is a schematic illustrating the structure of cup-stacked VGCNF). The nanofiber is clearly seen to have a hollow core surrounded by concentric cup-stacked planes. This functional structure has a large number of reactive edges both inside and outside the nanofiber [33,34]. Parallel layers in single layer VGCNFs were also observed using High resolution transmission electron microscopy (HRTEM) [30]. The d-spacing of the graphene sheets was reported as 0.34 nm (the same as that in MWCNTs and graphite platelets [35]).

As-produced VGCNFs are often formed of disordered graphene planes. Crystallinity of VGCNF can be enhanced by heat treatment of VGCNFs. Heat treatment enhances the nanofibers crystallinity by moving and re-arranging the carbon planes [1]. Optimum heat treatment conditions depend on the final desired properties. While graphitization (heat treatment at 2800 °C) of VGCNF having a stacked-cup morphology enhances the nanofiber crystallinity, it was found to degrade the nanofiber electrical and mechanical properties by changing the nanofiber morphology into discontinuous conical crystallite [8]. However, graphitization of VGCNF having a relatively disordered planes that are parallel to the fiber axis was found to enhance the nanofiber crystallinity and straighten the nanofiber planes along the fiber axis, as shown in Fig. 5 [1]. This morphology enhances the nanofiber mechanical properties due to the absence of grain boundaries. For the graphitized nanofiber Fig. 5b, a thin layer of amorphous carbon can be observed at the nanofiber surface as a result of the graphitization process.

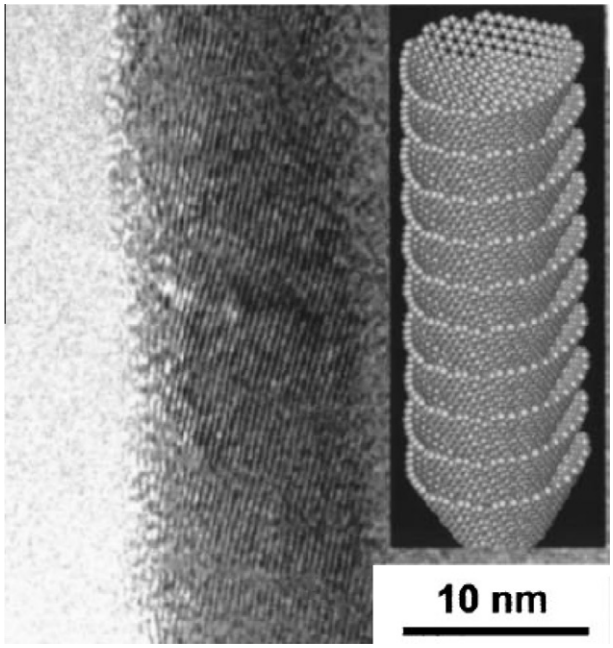

Fig. 4. HRTEM images shows a side-wall of a VGCNF having a cup-stacked structure. The inset is a schematic illustrates the cup-stacked structure [34].

2.2. Mechanical properties

Direct measurement of mechanical properties of nanofibers and nanotubes is technically difficult because of their small diameter [8]. Therefore, there are limited experimental data on the mechanical properties of nanofillers. Endo and coworkers [1] reported the mechanical tensile properties of sub-micron vapor grown carbon fiber (s-VGCF). The results showed that the tensile strength of graphitized s-VGCF increases with decreasing the fiber diameter, as shown in Fig. 6. For example, tensile strength of s-VGCF having a diameter of 100 and 300 nm were 2.2 GPa and 1.77 GPa, respectively. Fig. 7 shows tensile strength and tensile modulus of s-VGCF compared to different types of carbon fibers. It is apparent that the tensile strength and tensile modulus of s-VGCF is higher than that of general grade CF. On average, the tensile strength and tensile modulus of the s-VGCF are 2 and 200 GPa, respectively.

Tibbetts and Beetz [36] grew large diameter VGCFs and directly measured their tensile properties. Effect of fiber diameter on tensile properties was studied for the diameter range of 6.5–31.5 μm as shown in Fig. 8. One can clearly see that tensile properties decrease with increasing VGCF diameter. For a 7.5 μm diameter VGCF, the tensile strength and tensile modulus were 2.92 GPa and 237 GPa, respectively. However for a 31.5 μm in diameter VGCF, the tensile strength and tensile modulus decreased to 0.73 GPa and 120 GPa, respectively. Patton and coworkers [37] estimated the lower limit of the tensile modulus and tensile strength of Pyrograf® III VGCNF based on the rule of mixtures

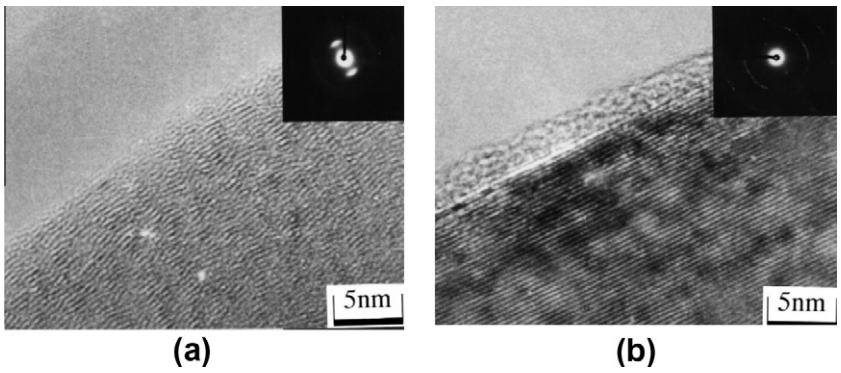

Fig. 5. TEM of a side wall of (a) as-grown VGCNF and (b) graphitized VGCNF [1].

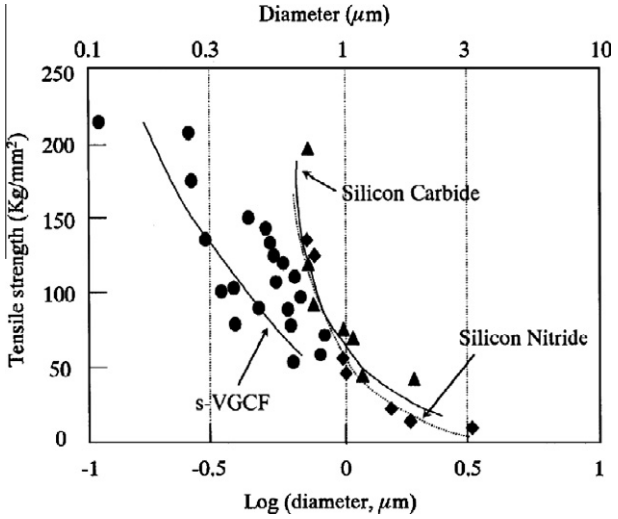

Fig. 6. Tensile strength of s-VGCF, SiN, SiC as function of diameter [1].

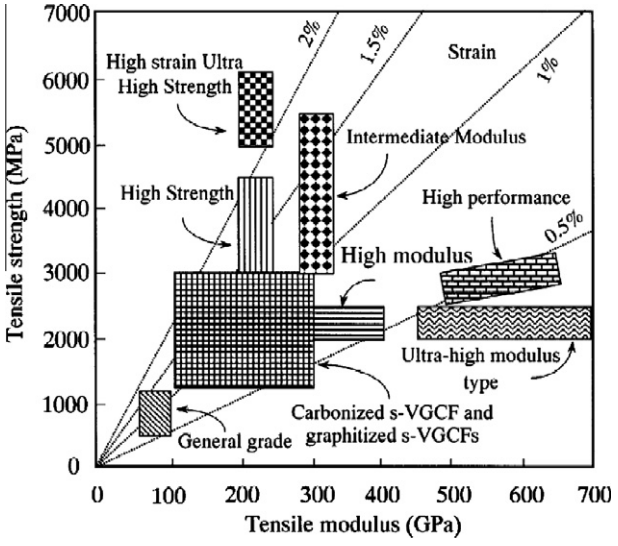

Fig. 7. Tensile properties of s-VGCF compared to those of various carbon fibers [1].

and experimentally measured mechanical properties of 15.5 vol% VGCNF reinforced epoxy. Their calculations revealed that the lower limit of tensile modulus and tensile strength are in the range of 88–166 GPa and 1.7–3.38 GPa, respectively.

Great efforts have been made to characterize the mechanical properties of CNTs [6,38]. Elastic modulus of CNTs have been mainly estimated by measuring intrinsic thermal vibration of the free ends of CNT using a TEM assuming that CNTs are clamped cantilever [39,40] and measuring load–displacement of cramped nanotube cantilever using AFM [41–43]. Using those techniques, elastic modulus values greater than that of graphite (1.02 TPa) have been reported for both SWCNT and MWCNT [39–43]. Such finding revealed that the current widely-accepted elastic modulus of graphite is underestimated [6]. Nevertheless, direct measurement of tensile properties of individual MWCNT prepared by non-catalytic arc evaporation showed that those nanotubes exhibit a tensile modulus in the range of 0.27–0.95 TPa [44]. The MWCNTs tested had an outer diameter, inner diameter and length in the range of 13–40 nm, 4–10 nm and 1.04–11.0 μm, respectively. No significant influence of the diameter on the elastic properties was reported. In the same study, MWCNT showed a fracture at strain and tensile strength of 12% and 11–63 GPa. Mechanical properties of chemical vapor deposition (CVD)-MWCNT, and consequently mechanical properties of VGCNF, are significantly lower than those of CNTs by the non-catalytic techniques because they have more defects. CVD-MWCNT may be considered a VGCNF with small diameter and a concentric perfect cylindrical graphene planes. Xie and coworkers measured the tensile properties of bundles of CVD-MWCNTs [45]. The average elastic modulus and tensile strength of CVD-MWCNT was estimated as 0.45 TPa and 0.36 GPa, respectively.

3. Mechanical properties

3.1. Background

In the previous section, the mechanical properties of VGCNF were presented. Tensile strength and tensile modulus of VGCNF were estimated to be at least two orders of magnitude higher than that of polymers. Thus, VGCNFs are promising mechanical reinforcement filler for polymers. Besides the filler intrinsic properties, mechanical properties of a polymeric composite material depend on many factors, including dispersion and distribution of filler, adhesion between filler and polymer matrix, filler aspect ratio and orientation of filler within the polymer matrix [46]. These factors are discussed in detail in the following sections.

3.1.1. Dispersion and distribution

Enhancing the mechanical properties of VGCNF composites requires good dispersion and distribution of nanofibers in the polymer matrix while maintaining the aspect ratio of nanofibers

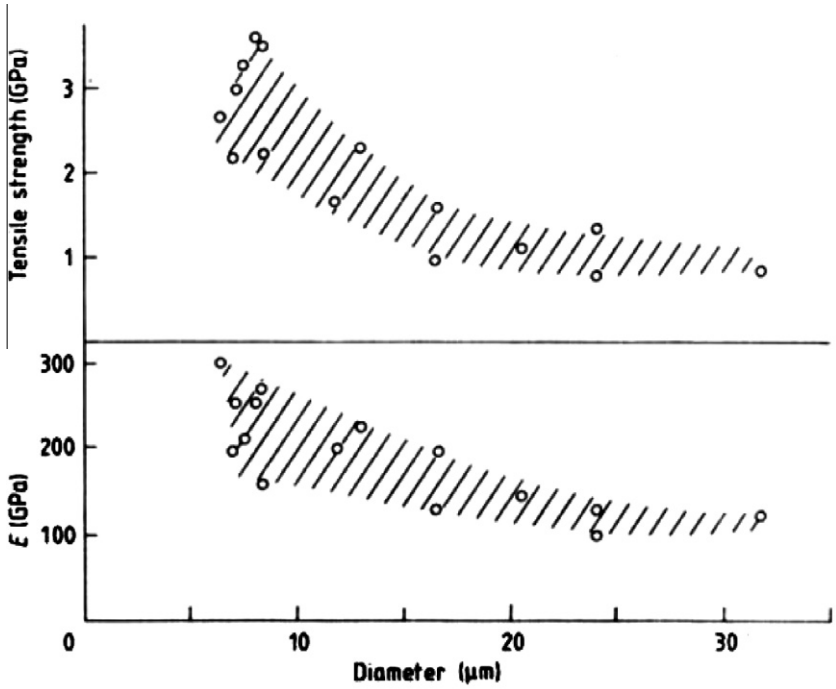

Fig. 8. Tensile strength and modulus of VGCF as function of diameter [36].

[24,47]. For a given polymer and filler, if the filler is not well dispersed within the polymer matrix, the composite will fail because of the separation of the filler bundle or agglomerate rather than the failure of the filler itself [48,49]. Excellent dispersion of filler minimizes the stress concentration centers and improves the uniformity of stress distribution [24]. Nanofiller can be dispersed and/or aligned in a polymer matrix using different techniques including in situ polymerization [50,51], solution processing [52,53], spin casting [54] and melt spinning [55,56]. In addition, some processing aids can be used to enhance the dispersion and/or alignment of VGCNFs such as sonication [57], surfactants [58], nanofiller functionalization or grafting [59,60] and magnetic fields [61]. In this section, we will only discuss the attempts that have been made to disperse VGCNFs in thermoplastic matrices using melt mixing techniques. Other techniques are discussed in the following sections along with their effects on the composites final properties.

Melt mixing is a simple and widely used composite compounding technique. Several reports have addressed VGCNF dispersion in thermoplastics by melt mixing [28,62–65]. However, this technique greatly reduces the filler aspect ratio especially in cases when high shear conditions are required to get adequate level of filler dispersion. For example, we found that melt mixing VGCNF with high density polyethylene (HDPE) in a HAAKE mixer at a moderate shear conditions (Torque 10 Nm, 50 rpm for 5 min) decreased VGCNF aspect ratio by 40% from 38 to 23 [28]. The average length of VGCNF 200 nm in diameter was reduced from 20–80 μm to 10.4 μm after melt mixing with PP in an extruder at 80 rpm and at a barrel temperature of 280–290 °C [66].

The severity of the mixing conditions that are required to disperse filler particles well in a polymer matrix depends mainly on the compatibility between the filler and polymer matrix. For example, VGCNF was dispersed in different polymer matrices (PP, polystyrene (PS), high impact polystyrene (HIPS) and acrylonitrile–butadiene–styrene (ABS)) using a Haake batch mixer [63]. Mixing at 80 rpm for 30 min was required to get good dispersion. However, we found that good dispersion of VGCNF (PR-24-LHT) in polyethylene (PE) can be achieved using a Haake batch mixer operated at 20 rpm for 15 min [12]. The reason for this difference can be related to the compatibility between the filler and polymer matrix (factors such as surface chemistry of VGCNF, polarity of the polymer matrix, surface tension of the filler and polymer influence the filler/polymer compatibility).

Grafting of fibers before melt mixing is a very promising modification process that can enhance the compatibility between the fiber and polymer matrix, and thus facilitating the dispersion of fibers in polymer matrix without implementing destructive shear mixing conditions. This process enhances the level of interaction between filler and polymer that consequently can improve the dispersion and distribution during mixing. CNTs dispersion in PP matrix was enhanced by using maleic anhydride grafted styrene-(ethylene-co-butylene)-styrene copolymer as a compatibilizer [27], and in poly(methyl methacrylate) (PMMA) by first coating CNTs with poly(vinylidene fluoride) (PVDF) before melt mixing [67]. It is out of the scope of this report to discuss the grafting techniques. Therefore, readers are referred to a recent review by Tsubokawa regarding polymer grafted carbon materials [68].

3.1.2. Adhesion and interface

To take full advantage of the superior tensile properties of reinforcement, such as VGCNFs and CNTs, requires excellent adhesion between the filler and polymer matrix to ensure adequate stress transfer [69,70]. Weak interfacial adhesion between the filler and polymer matrix increases the stress concentration at the filler/polymer interface leading to composite failure [71]. Stress transfer from a polymer matrix to filler might be directly from polymer to filler, or through an interfacial layer of polymer that has different characteristics than the bulk polymer (i.e. the matrix). Existence of such a layer complicates the analysis of composite fracture because of the introduction of new interfaces.

Many researchers reported the existence of such interfacial layers in composites [35,72,73]. In polycarbonate (PC)/MWCNT composites, MWCNTs sticking out from the fracture surface of a PC/MWCNT composite are covered with layers of PC in the range of 20–48 nm in thickness [72,73]. Coleman et al. [74] reported that

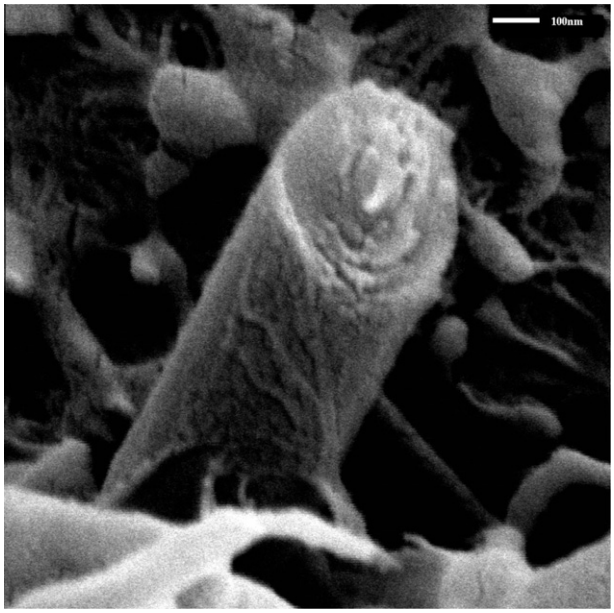

Fig. 9. SEM micrograph shows VGCNF coated with thick layers of HDPE. The scale bar is 100 nm [12].

the enhancement of tensile modulus of CNT/Polyvinyl alcohol (PVOH) composites exceeds that predicted by the parallel rule of mixtures (i.e. upper predicted bound). This unexpected result was attributed to the existence of ordered PVOH layer at the CNT surface that has better mechanical properties than the PVOH matrix [74]. According to a model developed in the same study, the tensile modulus of this interfacial layer is 46 GPa compared to 1.9 GPa for the pure polymer.

For HDPE filled with VGCNF, we observed interfacial layers of polymer covering VGCNFs extending out from the fracture surface of composite, as shown in Fig. 9 [12]. Fig. 10 is a histogram that shows the comparison of VGCNF diameters before and after mixing with HDPE. Details on the procedure followed to measure the nanofibers diameter before and after mixing can be found in reference [12]. The distribution shows that before mixing, 90% of VGCNF had a diameter below 150 nm, whereas after mixing 70% of the fibers had a diameter larger than 150 nm. Interestingly, the SEM observations illustrated that HDPE-coated-VGCNF has poor adhesion with the HDPE matrix as the gaps between the coated-fibers and the HDPE matrix can be clearly seen (see Fig. 11). Such observation reveals that the HDPE layers coating the VGCNF has different characteristics than the HDPE matrix.

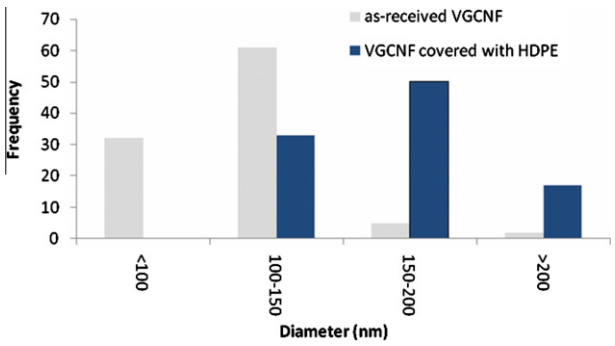

Fig. 10. Diameter size distribution of as-received VGCNF compared to that after processing with HDPE. (For interpretation of the references to color in this figure legend, the reader is referred to the web version of this article.)

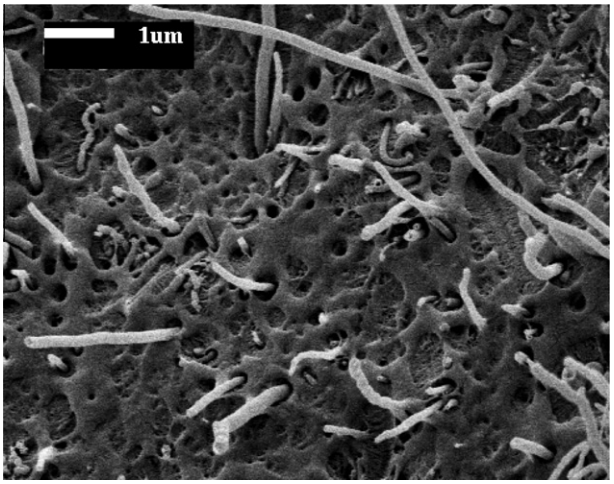

Fig. 11. SEM micrograph shows the poor adhesion between HDPE-coated-VGCNF and the HDPE matrix.

Adhesion between filler and polymer matrix could by physical, chemical and/or mechanical. Other forms of adhesion are diffusive and electrostatic but these are not common in polymer composites. Physical adhesion refers to the intermolecular forces, such as van der Waals forces, between filler and polymer matrix, which is the most common type of adhesion in polymer composites. Chemical adhesion represents chemical bonding, such as covalent bond, between the matrix and filler, which is typically the strongest form of adhesion. Filler particles are typically functionalized with certain chemical group in order to achieve good bonding with the polymer matrix. Mechanical adhesion represents the interlocking and entanglement of polymer chains within the filler structural voids and entanglement between filler functional chains and polymer matrix. Nanotubes and nanofibers with perfect cylinders of smooth surfaces exhibit insignificant mechanical interlocking with polymer matrix.

Adhesion between filler and polymer matrix can be quantified by measuring the interfacial shear strength (IFSS). Direct measurement of IFSS is not easy for nanofibers because of their small size. Nevertheless, Barber et al. [75] attached a single MWCNT on an AFM tip then embedded it into a molten polyethylene–butane. After solidifying the polymer, the MWCNT was pull-out using the AFM tip. The MWCNT used were 32–136 nm in diameter, which is comparable to the diameter range of VGCNF. The average IFSS was 47 MPa. This relatively high IFSS value revealed that there must be of covalent bonding between the filler and the polyethylene–butane matrix because molecular dynamics simulations by Frankland et al. [76] of ISFF between polyethylene and MWCNT showed an ISFF of 2 MPa. Fig. 12A shows a typical force vs. time curve for the pullout of a nanotube from a polymer matrix. Fig. 12B shows the geometry of the pullout area. Cooper et al. [77] used a scanning probe microscope (SPM) to pull-out single MWCNT extended from holes of MWCNT/epoxy film. IFSS up to 400 MPa was measured for MWCNT embedded (embedding length < 500 nm) in epoxy matrix. However, for MWCNT embedded to more than 500 nm, IFSS was in the range of 35–90 MPa.

3.1.3. Aspect ratio

Stress transfer from the polymer matrix to the filler increases with increase in the aspect ratio of filler [24,78]. Both Young's modulus and yield stress of clay/PA-6 composite was reported to increase with increase in the aspect ratio of clay [79]. Young's modulus estimation models for unidirectional short-fiber composites also predict increase in the modulus with increase in filler aspect

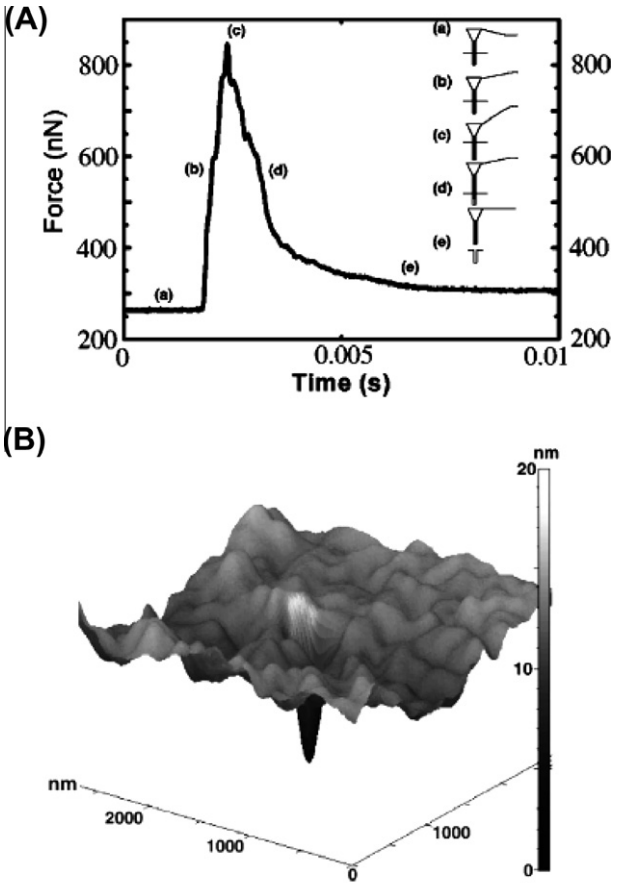

Fig. 12. (A) A typical figure shows the pullout force vs. pull out time as taken from the AFM cantilever deflection. (a) The nanotube is embedded in the polymer. As the nanotube is pulled away from the polymer, the cantilever bends away (b) until the maximum force, corresponding to the maximum cantilever bending deflection, is achieved (c). Pullout then occurs (d), resulting in the eventual complete separation of the nanotube from the polymer (e). (B) The geometry of the pullout area, clearly showing the hole previously containing the nanotube, is displayed from the AFM height data [75].

ratio [78]. When stress is imposed on a composite specimen, the stress will transfer to the fiber and build-up until it reaches the fiber tensile strength, at some critical distance x_c from the fiber end, where the fiber breaks. Thus, fibers shorter than the critical length ($l_c = 2x_c$ carry less stress than what they are supposed to based on their inherent mechanical properties. This means that their effective mechanical properties are lower than the inherent ones.

For hollow-core cylinders, such as the VGCNFs, the critical length is [35]:

$$l_c = \frac{\sigma_f D}{2\tau}\left[1 - \frac{D_i^2}{D^2}\right] \quad (1)$$

where σ_f is the fiber tensile strength, τ is the interfacial shear stress (IFSS), D and D_i are the external and internal diameters, respectively, of fiber. It is apparent that the critical fiber length decreases with decrease in the filler external diameter and tensile strength, and increases with decreasing interfacial shear strength and filler internal diameter. Filler internal and external diameters are typically characterized by TEM. Tensile strength of filler are either directly measured or can be estimated. IFSS is the most critical factor, since it depends on the adhesion between the filler and the polymer matrix. This level of adhesion can be very low such as 2 MPa between MWCNT and PE and very high such as the 400 MPa between MWCNT and epoxy matrix. For example,

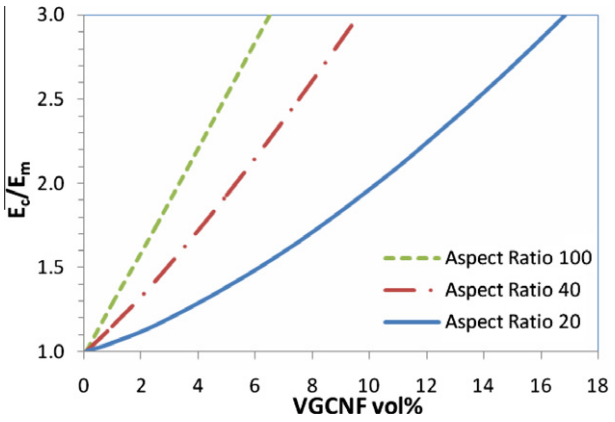

Fig. 13. Cox model predictions for the Young's modulus of VGCNF/polymer composites. (For interpretation of the references to color in this figure legend, the reader is referred to the web version of this article.)

according to Equation 1 for the case of poor adhesion between a VGCNF ($D_i = 30$ nm, $D = 70$ nm, $\sigma_f = 3$ GPa) and a polymer ($\tau = 2$ MPa), l_c is 43 μm. This length is much higher than the average length of VGCNF after mixing with a polymer, indicating that the fibers carry less stress than their actual capabilities. However, for the same fibers with good adhesion l_c drops to 0.2 μm (assuming $\tau = 400$ MPa).

3.1.4. Theoretical predictions of tensile properties

Young's modulus of VGCNF/polymer composite as a function of VGCNF volume fraction and aspect ratio was estimated using the Cox model [80,81]:

$$E_c = (1 - V_f)E_m + nV_f(\eta_f E_f) \quad (2)$$

$$\eta_f = 1 - \frac{\tanh\beta}{\beta} \quad (3)$$

$$\beta = \frac{l}{d}\sqrt{\frac{E_m}{(1+\nu)E_f \ln\sqrt{\left(\frac{\pi}{4V_f}\right)}}} \quad (4)$$

where E_c is the composite Young's modulus, V_f is the volume fraction of the filler, E_m is the Young's modulus of the polymer matrix, η_f is the filler efficiency factor, E_f is the filler Young's modulus, n is a constant related to the orientation of the fibers ($n = 1/6$ for randomly oriented fibers in 3-D, $n = 1/2$ for fibers randomly oriented in 2-D plane and $n = 1$ for aligned fibers), l is the average fiber length, d is the fiber diameter, and ν is the Poisson's ratio.

The Cox model is an extension of the parallel model based on the rule of mixtures. Cox introduced a filler efficiency factor to the parallel model to account for the effect of filler aspect ratio on stress transfer [80]. The parallel model was originally developed for composite specimens in which fibers are aligned in the tension direction and span the entire length of the specimen, whereas, in actual composites, fibers are much shorter than the specimens.

Fig. 13 depicts the influence of VGCNF aspect ratio and volume fraction on the Young's modulus of VGCNF/polymer composite as predicted by the Cox model. The calculation is for a randomly oriented VGCNF ($E_f = 240$ GPa) in polymer matrix having a Young's modulus of 1 GPa and a Poisson's ratio of 0.38. It is clear that the amount of VGCNF required to double the Young's modulus decreases significantly from 10 vol% to 3.5 vol% with increasing the VGCNF aspect ratio from 20 to 100. In a previous work we found that the aspect ratio of (PR-24-LHT) VGCNF after mixing at 50 rpm for 5 min is about 20 [28].

3.2. Tensile properties of VGCNF/polymer composites

Only marginal improvements in tensile properties were achieved when as-grown VGCNF were incorporated into polymer matrices when there was no functionalization of nanofibers or attempts to enhance their dispersion or orientation in the composites [82,83]. Moreover, at high filler loading, the poor dispersion of nanofibers deteriorated some composite mechanical properties. For example, VGCNF/poly(ether ether ketone) (PEEK) composites prepared by extrusion followed by injection molding showed linear increase in tensile modulus and yield stress with increasing VGCNF loading [84]. At 15 wt% VGCNF loading, the tensile modulus and yield stress of the composite increased by 40% and 15%, respectively, over that of unfilled PEEK. Surprisingly, adding up to 10 wt% VGCNF to PEEK had very little effect on the strain at break; the strain at break value only reduced from 22% to 18%. Similar observations were also found by Shui and Chung [85] for poly(ether sulfone) PES filled with carbon filaments filled, where at 5 vol% and 7 vol% VGCNF, strain at break only dropped by 19% and 31%, respectively. In contrast to this, Lozano and Barrera reported 60% and 73% drop in strain at break for 5 and 10 wt% VGCNF filled PP, respectively [86].

Before going in depth about the tensile properties of VGCNF/polymer composites, some of the typical tensile strength and tensile modulus properties that have been reported for VGCNF/PP composites are presented in Figs. 14 and 15, respectively. It is apparent that for all of the VGCNF/PP composites regardless of the processing method, there is a linear increase in tensile strength with increasing VGCNF content up to 5 vol%. Beyond that, adding VGCNF has little influence on tensile strength. The most remarkable increase in tensile strength was obtained by Gordeyev and coworkers [87] who prepared the VGCNF/PP composites by traditional fiber processing technique. For the Young's modulus, it can observed that for most of the studies on VGCNF/PP composites, 7–8 vol% VGCNF were required to double the composite stiffness.

In order to enhance the mechanical properties of VGCNF/polymer composites, different methods have been developed to disperse and distribute VGCNF well in the polymer matrix and to

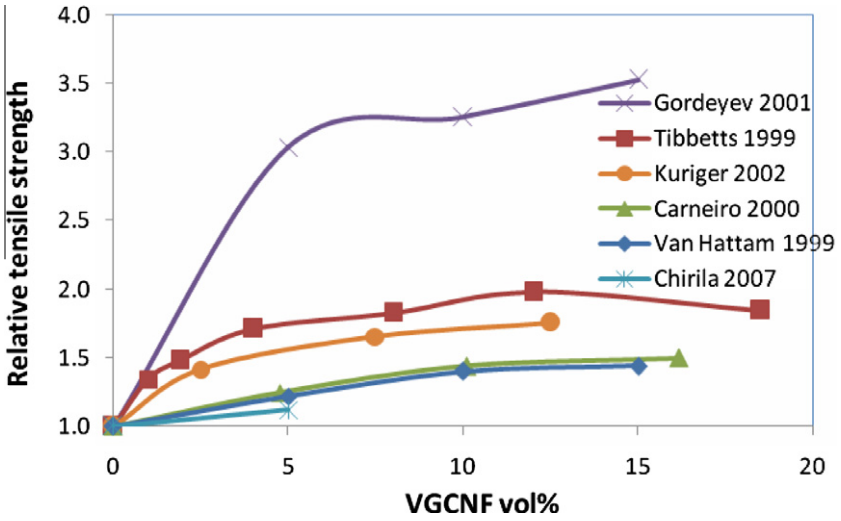

Fig. 14. Tensile strength of VGCNF/PP composites obtained by different researchers. (For interpretation of the references to color in this figure legend, the reader is referred to the web version of this article.)

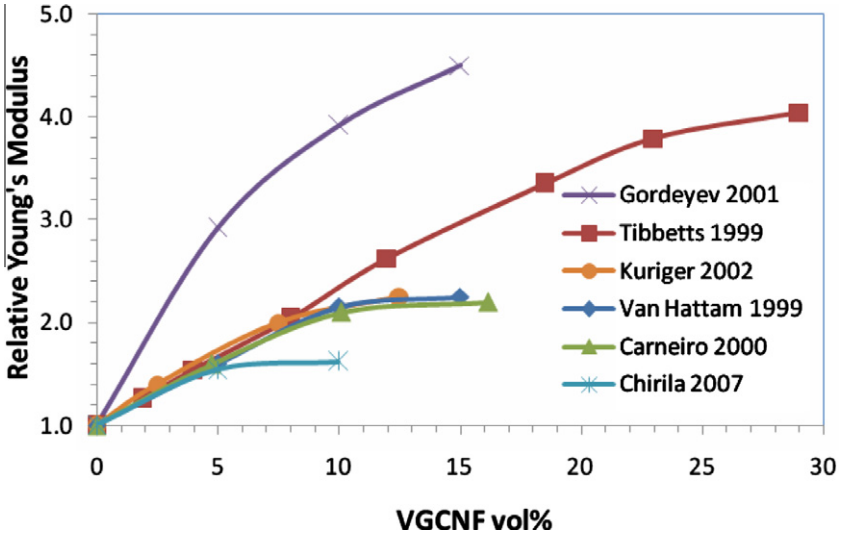

Fig. 15. Young's modulus of PP/VGCNF composites obtained by different researchers. (For interpretation of the references to color in this figure legend, the reader is referred to the web version of this article.)

enhance the adhesion between nanofibers and polymer matrix. These methods are reviewed in the following sections.

3.2.1. Ball milling treatment

Remarkable improvement in tensile properties of VGCNF/PP and Nylon composites compounded in a MiniMax Molder were reported after ball milling the VGCNF [88]. The Mini-Max molder (Custom Scientific Instruments, Inc.) is a gram scale mixer. Its mixing efficiency in terms of filler dispersion and distribution is lower than that of internal mixers and extruders because of its simple flow patterns [89–93]. Ball milling the VGCNF clumps prior to composite compounding facilitated the infiltration of polymer into VGCNF agglomerates and consequently enhanced the mechanical properties of both nylon and PP composites. The Influence of ball-milling on tensile strength was more pronounced than its influence on tensile modulus. For example, balling milling increased the tensile strength of 4 vol% VGCNF/PP composite from 28.5 to 47.5 MPa, corresponding to 67% increase, whereas, it increased the tensile modulus from 1900 to 2450 MPa, corresponding to only 29% increase. Data from Tibbetts (1999) in Figs. 14 and 15 are for the tensile strength and tensile modulus, respectively, of ball-milled VGCNF/PP composites.

3.2.2. Surface treatment

Adding oxygen to the surface of VGCNF is an effective method to enhance the adhesion between the carbon nanofiller and polymer matrix. Oxygen has been added to the surface of VGCNF by etching the nanofiber in air at about 400–600 °C, soaking the nanofibers in nitric acid, sulfuric acid or sulfuric/nitric acid mixture [8,94], and by oxygen plasma treatment [82,95,96]. Adding polar functional groups to the surface of nanofibers increases the surface energy (especially the polar part) of the nanofibers. Thus, the degree of functionalization can be simply characterized by water contact angle measurement. The smaller the contact angles the higher the functionalization [95,96].

Four types of functional groups are generated in oxygen plasma treatment; namely, carboxylic, carbonylic, phenolic or hydroxylic groups [95,96]. At a certain surface energy, the ratio of polar to dispersive surface energy can be optimized by adjusting the plasma power and treatment time. Lower plasma power and longer treatment time are needed to increase the value of polar surface energy [95,96]. At 2.3 vol% VGCNF, tensile properties of plasma-treated VGCNF/PP composite were marginally higher than the untreated-VGCNF/PP composite and the neat PP. However, adhesion between plasma treated nanofibers and PP matrix was better compared to that between untreated fibers and PP matrix [95,96]. Such low levels of improvement can be ascribed to either the poor dispersion of nanofillers in the PP matrix or most likely to the low concentration of VGCNF. Similarly, different levels of HNO_3 treatment of VGCNF did not increase the tensile properties of 2.3 vol% VGCNF filled PP [97]. In addition to adding oxygen functional groups to the surface of nanofiller, oxidation also reduces the aromatic concentration on the surface nanofibers. The required degree of oxidation depends on the hosting polymer. For PP, modest covering of the nanofibers surface (around 4%) with oxygen gave a composite with optimum tensile strength [8,98]. However, for epoxy, more highly oxidized surface of nanofibers is required [8].

VGCNF used in the previous studies are expected to have an aspect ratio between 20 and 40. Thus, higher volume fraction of this filler should be used to enhance the composite mechanical properties. This conclusion is consistent with the considerable improvements in tensile properties of PP filled with 15 vol% air etched or CO_2 etched VGCNF. For example, tensile strength of air-etched VGCNF composite was at least two times that of composites prepared using as-grown or graphitized VGCNF [98]. The adhesion between the air-etched fibers and the PP matrix was better than that between the graphitized VGCNF and the PP matrix (see Fig. 16). The figure shows that the pulled-out nanofibers from the fracture surface of graphitized-VGCNF/PP composite is much longer than those from the air-etched VGCNF/PP composite indicating better adhesion between the nanofibers and polymer for the latter composite.

3.2.3. VGCNF alignment

Alignment of nanofibers in polymer matrix was attempted by extrusion through a die [66], spinning [65,87,99] and freeform fabrication [100,101]. The best reinforcement results were obtained by Gordeyev and coworkers [87] who addressed the possibility of incorporating VGCNF into the fibrillar structure of semi crystalline polymer because of their nanometer-size. Upon stretching at high temperature, most semicrystalline polymers can form fibrillar structure to self-reinforce. VGCNF/PP composites samples were spun and then stretched at different draw ratios. The composite were prepared by extrusion. For as-spun samples with draw ratio (DR) of 1–1.5, the relative tensile strength and relative tensile modulus of the 5 vol% VGCNF composite were 3.1 and 2.9, respectively. Increasing VGCNF content above 5 vol% had a marginal effect on the as-spun samples drawn at 1–1.5. Fig. 17 shows the influence of DR and VGCNF loading on the tensile strength and stiffness of the VGCNF/PP composites. The highest tensile strength and tensile modulus reported were 720 MPa and 14.9 GPa, respectively, for 5 vol% VGCNF/PP composite spun and then stretched to total DR of 15. The tensile strength and modulus for unfilled PP processed under the same conditions were 530 MPa and 8.3 GPa, respectively.

Poor tensile properties were obtained from spinning 5 wt% VGCNF/poly(ethylene terephthalate) (PET) composites [99]. The composites were prepared by melt mixing in an internal mixer or twin screw extruder. Tensile strength either stayed at the same value or decreased with addition of VGCNF depending on the type

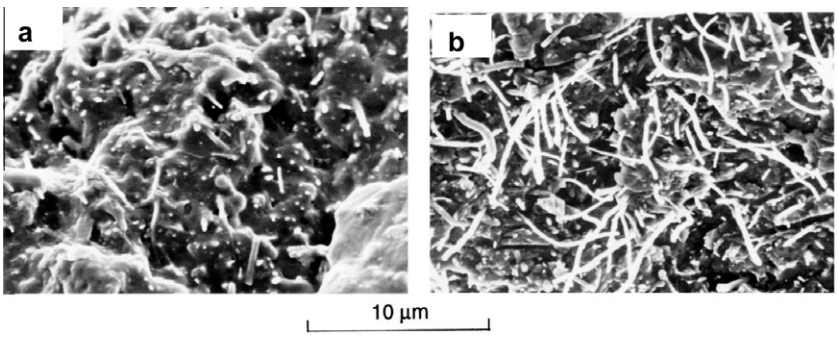

Fig. 16. SEM micrographs of (a) air-etched VGCNF/PP composite; (b) graphitized VGCNF/PP composite [98].

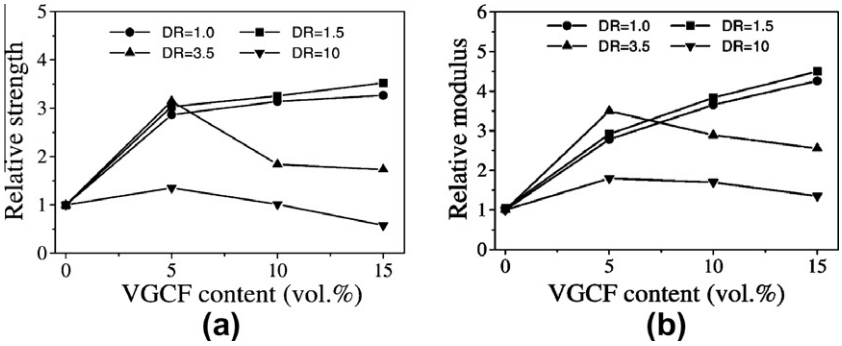

Fig. 17. Effect of VGCNF loading and draw ratio on the as-spun (DR = 1–3.5) and drawn (DR = 10) VGCNF/PP composites (a) relative strength and (b) relative modulus [87].

of VGCNF and processing conditions. However, compressive strength and torsional modulus of composites were higher than that of unfilled polymer fiber by up to 50% and 57%, respectively. Improvement in the tensile modulus of VGCNF/PMMA composite was obtained by spinning [102]. 0, 5 and 10 wt% VGCNF/PMMA composite were processed in a piston-driven spinning system having an orifice diameter of 4 mm. Fibers with 2 different diameters, 4 mm and 60 μm, were obtained. The 4 mm fibers were collected as they came from the spinning system (i.e. no drawing), whereas the 60 μm fibers were collected by drawing the outlet of the spinning system at 150 m/min. The stiffness of the 60 μm fibers was 2–3 times that of the 4 mm fibers. However, the tensile strength decreased by 25% by introducing the nanofibers. Marginal increase in tensile strength was found by partial alignment of VGCNF in PP matrix via extrusion through a converging-annular die [66]. Nanofiber alignment in the extrusion direction decreased with increasing fiber content. Enhancing nanofiber alignment was possible by increasing the residence time in the die channel. The flexural strength of 15.5 vol% VGCNF/epoxy composite processed in two-roll mixer after mechanical blending was marginally higher than that prepared by only mechanical stirring [37]. The two-roll mixer was found to reduce the void content and it is expected that it produces a composite with better nanofiber alignment.

Extrusion freeform fabrication (EFF) technique was utilized to reorient VGCNF and SWCNT in an ABS matrix [101]. The composites were first prepared by melt mixing in an internal mixer, from which randomly oriented nanofibers were obtained. Those composites were divided into two parts. The first portion was hot molded and then cut to obtain dog bone-shaped specimens for tensile testing. The second portion was further processed by EFF to produce fibers and dog-bone tensile bars for tensile testing. In the EFF, the part is sliced into layers of finite thickness using a 3D computer program. Then the EFF machine builds the part layer by layer. This type of fabrication allows the manufacture of complex geometries [100]. After EFF processing, both VGCNF and SWCNT filled ABS showed some degree of nanofiber alignment. Tensile testing results illustrated that 5 wt% VGCNF or SWCNT filled ABS composites prepared by hot molding (the first portion) have marginally higher tensile strength (9% and 21%, respectively) and modulus of elasticity (22% and 29%, respectively) than unfilled ABS. For EFF composites having dog-bone shape, no enhancement in tensile strength was reported and marginal increases in tensile modulus were found (9% and 26%, respectively). These unexpected tensile properties after filler alignment were attributed to the in-layer void and incomplete inlayer fusion in the EFF. Finally, for the EFF fibers, for both VGCNF and SWCNT composites a significant improvement in tensile modulus by 44% and 93%, respectively, was reported.

3.2.4. Processing methods and processing conditions

Processing methods and processing conditions have significant influence on the parameters (filler distribution, dispersion, orientation and aspect ratio) that determine the mechanical properties of a polymer composite. Due to the poor adhesion between VGCNF and HDPE, changing mixing conditions in an internal batch mixer has little effect on the mechanical properties of 7.5 vol% VGCNF/HDPE composite [64]. Similarly, the effect of extrusion condition on tensile properties of PP filled with 0–12.5 vol% VGCNF was not significant [103]. The extrusion temperature was varied from 215 to 250 °C and screw speeds were 40 rpm and 120 rpm. The void content decreased with increasing processing temperature and/or decreasing filler content. Both tensile modulus and ultimate tensile strength increased with increasing VGCNF content, except for the composites prepared at 215 °C, where increasing VGCNF content from 7.5 to 12.5 vol% did not affect tensile strength. Relative tensile strength and relative tensile modulus of 12.5 vol% VGCNF reinforced PP composite were 1.8 and 2.2, respectively. Tensile properties of VGCNF/PMMA composites prepared by chaotic mixer and internal mixer surprisingly showed a marginal decrease in Young's modulus and even more disappointing and more remarkable decrease in stress at break upon adding only 0.5 wt% VGCNF [29]. For example, the stress at break for the composite prepared in the internal mixer decrease from 52 MPa for pure polymer to 30 MPa for 0.5 wt% VGCNF filled polymer.

Patton and coworkers [37] studied the mechanical properties of VGCNF filled epoxy as a function of processing method and processing conditions. For 18.2 vol% VGCNF/epoxy composites prepared by acetone/epoxy infusion in a mat of nanofibers under

Table 2
Best tensile properties results reported for CNT–polymer composites prepared by different methods (adapted from Ref. [24]).

Polymer	Method	CNT type	CNT (wt%)	Relative modulus	Relative strength	Ref.
PVA	Solution processing	MWCNTs	1	3.6	4.3	[105]
PA-6	Melt mixing	MWCNTs	2	3.1	2.6	[106]
PP	Spinning	SWCNT	5	3.5	3.2	[107]
PMMA	In situ polymerization	MWCNTs	1.5		1.75	[108]
PEI	Layer by layer deposition	SWCNTs	50	36.7	24	[109]
PA-6	Melt spinning	PA6g-SWCNTs	1.5	2.7	2.1	[110]

vacuum followed by curing, increasing curing pressure from 14.7 to 250 psi improved the flexural strength and flexural modulus by 30% and 5%, respectively. Increasing curing pressure beyond 250 psi negatively influenced the flexural properties.

3.2.5. Tensile properties of CNT/polymer composites

After reviewing the tensile properties of VGCNFs/polymer composites, in Table 2 some of best tensile properties reported so far for CNTs/polymer composites are summarized. Recently, a more comprehensive list was published by Spitalsky and coworkers [104]. The objective from presenting this table is to give the reader a numeric comparison between the tensile properties of VGCNFs/polymer composites to those of CNTs/polymer composites. It is clear that compared to VGCNFs/polymer composites, CNTs/polymer composites have better tensile properties at lower filler loading. This can be attributed to the better tensile properties of CNTs compared to VGCNFs. However, it should be mentioned that CNTs/polymer composites have received much more interest than VGCNFs/polymer composite and thus much more work has been conducted to improve CNT/polymer composite properties. For example, the effect of VGCNF grafting on the tensile properties of VGCNF/polymer composites has not been studied yet. More studies need to be done to evaluate the tensile properties of VGCNF. Better understanding of the effect of VGCNF structure and dimensions on composite properties also requires study. There also needs to be emphasis on synthesizing nanofibers with better mechanical properties.

3.3. Fracture toughness

Miyagawa and Drzal [111] studied the fracture toughness of plasma-treated-VGCNF/epoxy and untreated-VGCNF/epoxy composites. It was found that the fracture toughness of untreated VGCNF/epoxy increased remarkably with increasing filler loading, and at any filler loading, it was higher than that of plasma treated-VGCNF/epoxy. This was attributed the poor adhesion between the untreated fibers and epoxy matrix which dissipated larger energy during the fibers pull out process. However, for treated VGCNF/epoxy composites, the good adhesion between the fibers and epoxy matrix resulted in failure due to fiber breaking. Thus, the energy absorbed during breaking was smaller than that required for pull out of the fibers [111]. The model is schematically described in Fig. 18.

3.4. Dynamic mechanical properties

Incorporating VGCNF into epoxy matrix was found to enhance the storage modulus of the composites [111] around and above the T_g [47], as shown in Fig. 19a. More interestingly, storage modulus of a composite prepared using low viscosity epoxy was higher than that of a composite prepared using high viscosity epoxy, because of the better dispersion of VGCNF and less void volume fraction in the low viscosity epoxy composite [47]. Increasing VGCNF loading in PC matrix was found to increase the storage modulus below the T_g, as shown in Fig. 19b. For PMMA/VGCNF composites prepared at low temperatures by a chaotic mixer, a remarkable increase in storage modulus was found by increasing VGCNF from 0 to 1 wt% [29]. However, the storage modulus deteriorated when VGCNF loading increased from 1 to 4 wt%. At 4 wt% VGCNF, the composite storage modulus was below that of unfilled PMMA. For PMMA/VGCNF composites prepared by internal mixer, a minor influence on storage modulus by changing VGCNF loading from 0 to 4 wt% was reported. Such observations for VGCNF/PMMA

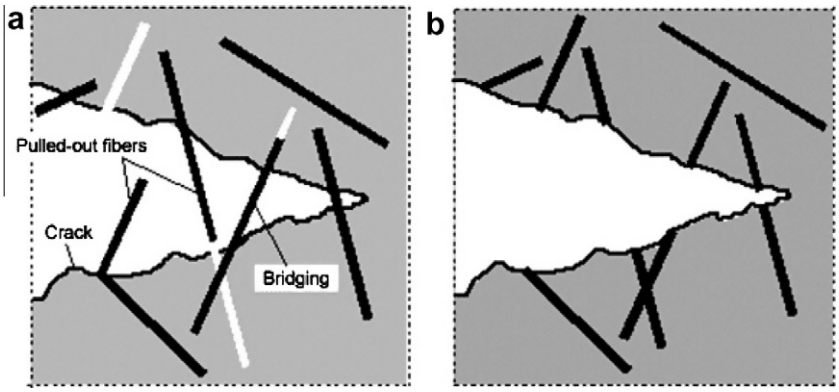

Fig. 18. Propagation of crack model for VGCNF/epoxy composites with: (a) poor adhesion and (b) good adhesion [111].

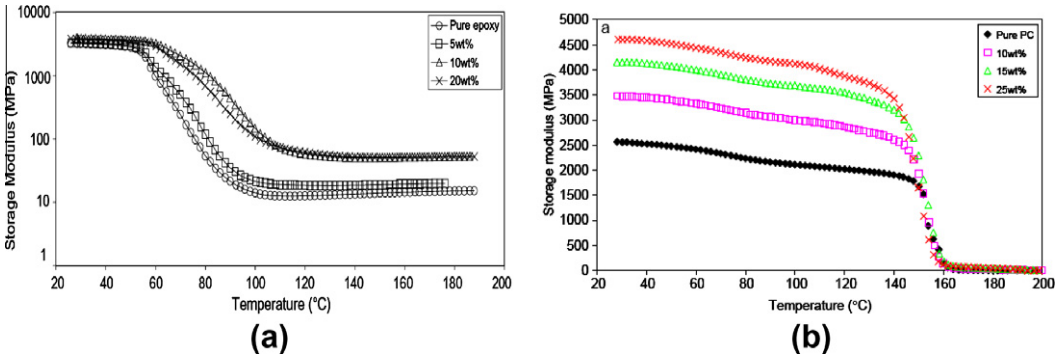

Fig. 19. DMTA of (a) VGCNF/epoxy composites [47] and (b) VGCNF/PC composite [112]. (For interpretation of the references to color in this figure legend, the reader is referred to the web version of this article.)

composites might be due to a state of poor dispersion of nanofiber within the polymer matrix.

4. Rheological properties

Rheological analysis of polymer composites is an efficient method to predict the processing behavior and microstructure (dispersion, distribution, concentration of filler and adhesion between filler and polymer matrix) of composites [72,113–121]. Many polymer composites showed transition in rheological behavior from liquid-like to pseudo-solid-like or solid-like with increasing filler concentration. The transition concentration is called the rheological percolation threshold. In the liquid-like region, the rheological properties are dominated by the polymer–polymer entanglements and characterized by storage modulus (G') proportional to the square of angular frequency, i.e. ($G'\alpha\omega^2$). In the solid-like region, the rheological properties are a response to a combination of polymer–polymer entanglements, polymer–filler interactions and filler–filler interactions. The solid-like region is characterized by G' of ω, and G' remarkably higher than the loss modulus G'' [122,123]. For the pseudo-solid-like region, the system is similar to but does not completely fulfill the solid-like behavior. For example G' may be independent of ω but not remarkably higher than G'' [122].

The rheological percolation is fundamentally different than the electrical percolation threshold. Electrical percolation is the concentration at which conductive filler particles form a continuous filler network in the polymer matrix, such that, at the electrical percolation threshold, the composite electrical conductivity suddenly increases by several orders of magnitude (up to 10^{15} S m^{-1}). However, for the rheological percolation threshold no dramatic increase in G' or complex viscosity η^* occurs. The onset of rheological percolation can be characterized, for example, by significant change in the slope of the G' vs. concentration or in the slope of η^* vs. concentration curves. Fig. 20 shows the electrical and rheological behavior of MWCNT/PC composite. It is apparent that at the electrical percolation threshold, between 1 and 2 wt%, the electrical resistivity decreased by several orders in magnitude. However, for the rheological percolation threshold, which can be identified at low frequencies, the significant change in η^* slope starts ~1 wt%. From 1 to 5 wt% MWCNT, there is a linear increase in the log (η^*) with increase in concentration.

The rheological percolation threshold concentration depends on the measurement temperature. Thus, it can be higher, equal to or lower than the electrical percolation threshold. Generally speaking, the rheological percolation threshold decreases with increase in temperature indicating that not only the filler–filler interaction but also combination of polymer–filler and polymer–polymer networks determine the rheological properties [114]. Kelarakis et al. [122] characterized the critical gel point (system transition from pseudo-solid-like to liquid-like behavior), i.e. the rheological

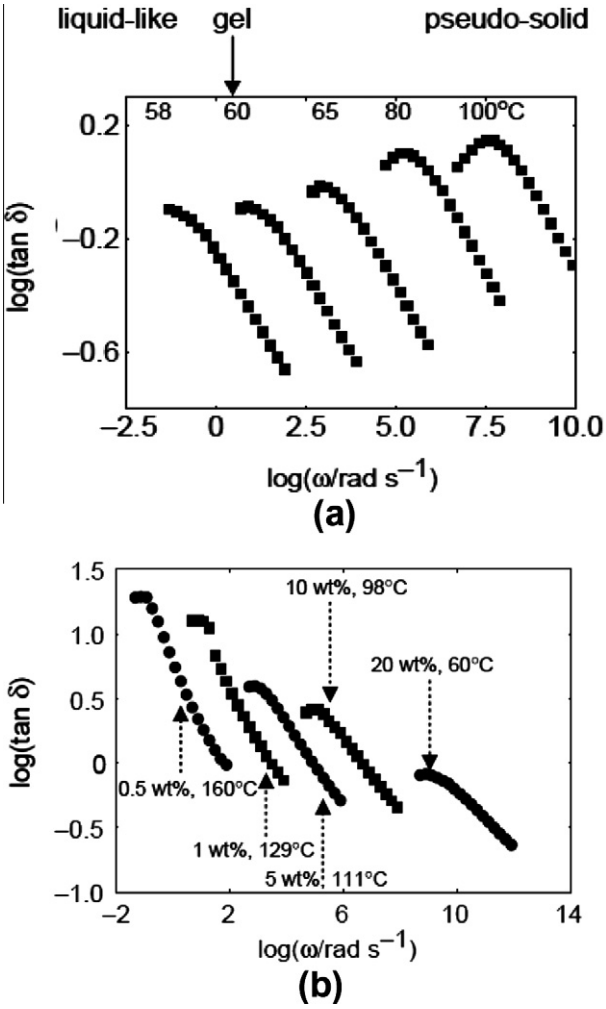

Fig. 21. (a) tan δ curves as a function of frequency and temperature of 20 **wt%** MCNF/EP composite. Gel point is indicated by the arrow. (b) tan δ curves at the gel point for various MCNF/EP composites as a function of filler concentration [122].

percolation threshold temperature, of modified carbon nanofiber (MCNF)/ethylene–propylene (EP) copolymer composite using the Winter–Chambon criterion [124,125]. The criterion suggests that the critical gel point is the temperature at which the tan δ vs. ω curve exhibit a zero-slope at low frequency [122]. Fig. 21a shows the temperature dependence of the slope of the tan δ curves of 20 wt% MCNF composite at low frequencies. It is apparent that tan δ curve exhibits a zero-slope at 60 °C. Above 60 °C, the composite is clearly seen to exhibit a pseudo like-solid behavior, where the slope of the tan δ curves at low frequencies is positive. Fig. 21b

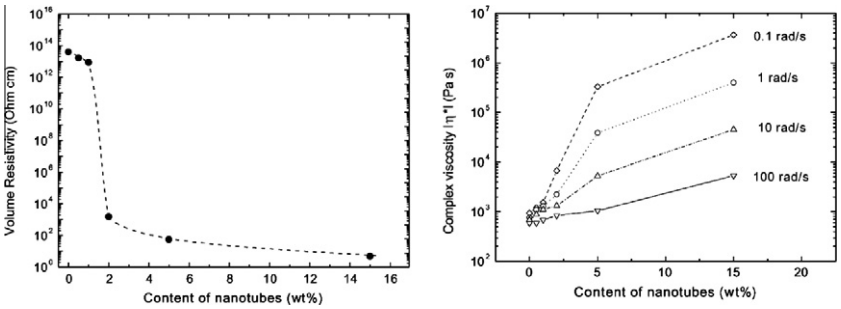

Fig. 20. (a) Electrical percolation threshold and (b) rheological percolation threshold of MWCNT/PC composite [72].

shows the gel point curves at various filler concentrations. It can be clearly seen that gel point significantly decreases with increase in filler concentration.

Very few studies have been performed on the rheological behavior of VGCNF/polymer composites. VGCNF/PE composites exhibited increase in storage modulus and loss modulus with increase in VGCNF loading [126]. The increase in storage modulus was more significant than that in loss modulus. Both unfilled-PE and VGCNF/PE composites showed typical shear thinning behavior. At high frequencies, the difference in viscosity between neat and highly filled composites was very small. Similar observation was reported for VGCNF/PP composites [62]. For PC composites, at shear rates less than 0.1 s^{-1}, adding 10 wt% VGCNF had very small influence on complex viscosity of VGCNF/PC composites [127]. However, at shear rates greater than 0.1 s^{-1}, the complex viscosity of the composites decreased with increasing VGCNF loading and was lower than that of neat PC. This phenomenon was also reported in CB filled PS systems characterized at 230 °C [128]. At high temperatures, PS is Newtonian over a wide range of frequencies. This implies that the polymer chains are not entangled. Therefore, adding CB facilitates the chains movements by acting as ball-bearings [129]. We believe that same analysis applies for VGCNF/PC composites, since PC is nearly Newtonian at shear rate up to 100 s^{-1}. For MWCNT filled PC, it has been reported that melt viscosity increases with increasing MWCNT loading. Composites with lower viscosity than neat polymer were not noticed [72,130].

Carneiro and Maia [127] compared the rheological properties of sub-micron VGCF/PP and CF/PP composites. At low shear rates, the complex viscosity of 30 wt% VGCF/PP was two orders of magnitude higher than that of 30 wt% CF/PP. 30 wt% VGCNF/PP composite exhibit a typical shear thinning behavior over the entire range of shear rates studied (0.001–10,000 s^{-1}); whereas, both unfilled PP and 30% CF filled PP exhibited a Newtonian plateau at shear rates below 0.1–1 s^{-1}. The strong shear thinning behavior of VGCNF/PP composites was attributed to the existence of fiber–fiber interactions. In the same study, it was found that increasing mixing intensity, by changing screw configuration caused a very small decrease in the composite viscosity. The decrease was clearly seen only at low shear rates and the decrease was mainly because of the decrease in nanofiber length. Increasing composites viscosity with increasing filler aspect ratio was reported for both GF and CF filled composites [129]. The higher the aspect ratio, the more pronounced is the interaction between fibers.

5. Crystallinity and T_g

Depending on the type of polymer matrix and filler concentration, addition of nanofiller can either increase or decrease the crystallinity [46]. For VGCNF/PE composite, a reduction in PE crystallinity was reported by adding VGCNF [46]. However, an increase in PP crystallinity, crystallization temperature and crystallization rate were reported with increasing VGCNF content. Even though PC has a very slow crystallization rate, Takahashi and coworkers [131] reported that addition of graphitized-VGCNF to PC accelerates the crystallization of PC. From DSC analysis of VGCNF/PC composite annealed at 200 °C for 2 h, an endothermic peak was observed at 234.6 °C. Under the same annealing condition, no signs of crystallinity were observed when non-graphitized VGCNF were used. Zhang and coworkers [132] found that addition of 1.5 phr VGCF to HDPE or (50/50) HDPE/PMMA blend reduces the Ozawa's exponent.

Effect of VGCNF addition on glass transition temperature of polymers was found to be dependent on the interaction between the nanofiller and the polymer matrix [2]. No influence on the T_g of VGCNF/PS was observed with addition of up to 10.6 wt% of VGCNF [133]. Similar observation was also noted for MWCNT/Poly (styrene-co-butyl acrylate) filled with up to 15 wt% MWCNT [134]. Both of the aforementioned composites were prepared by hetero-coagulation. Similar observations were reported for VGCNF/PEEK composite prepared by melt mixing [84], and VGCNF/PC composite prepared by melt mixing [112]. However, the tan δ peak decreased with increasing VGCNF content due to reduction of polymer concentration [112]. However, Zeng and coworkers [102] found that glass transition temperature of VGCNF/PMMA spun fibers is 5 °C higher than that of a controlled PMMA sample (PMMA processed under similar conditions before testing). Similar observations were reported for VGCNF/epoxy composites [47,135,136]. Introducing 5 wt% VGCNF to epoxy has small effect on the T_g and the tan δ peak. However, by increasing VGCNF loading to 10 wt%, a significant increase in T_g (T_g increased from 80 to 100 °C) and decrease in the height of tan δ peak was noticed [47]. The presence of VGCNF restricts the segmental movement of the polymer chains, and thus results in an increase in T_g.

6. Summary and conclusions

VGCNFs are promising nanofillers for several applications due to their multifunctional characteristics. VGCNFs are produced by chemical vapor decomposition of a hydrocarbon feedstock on a metal catalyst. VGCNFs are typically 50–200 nm in diameter and up to 100 μm in length. The nanofiber has a hollow core compromised of single or double layers of graphene planes stacked parallel or at a certain angle from the nanofiber axis. The low price of VGCNFs compared to competitive fillers such as CNTs will be one of the major determinants of their widespread commercial use in the polymer industry. VGCNF/polymer composites have potential applications in many fields including: structural, EMI SE, ESD protection, batteries, sensors and automotive industry. In addition, VGCNF are good substitute of CFs and CB in many applications.

Good dispersion, uniform distribution, high VGCNF aspect ratio and strong adhesion between VGCNF and polymer matrix are they key factors for producing multifunctional VGCNF reinforced polymer composites with outstanding mechanical properties. Since melt mixing is the most favored method for composites compounding, functionalizing nanofibers, feeding nanofibers after the polymer pellets have melted, avoiding high-shear mixing conditions and/or using a compatibilizer are essential approaches to facilitate the dispersion and distribution of nanofibers and to retain the high aspect ratio of VGCNF.

Mechanical properties of VGCNF/polymer composites are lower than those of CNT/polymer composites. One reason is the better intrinsic mechanical properties of CNTs over VGCNFs. This clearly indicates that producing VGCNFs with better mechanical properties is required to formulate a multifunctional VGCNF/polymer composite at lower filler loading. The best tensile properties of VGCNF/polymer composites reported so far were for VGCNF/PP composites obtained by melt spinning. For composites prepared by melt mixing and many other techniques, 10 vol% of VGCNF were required to double the tensile strength and tensile modulus. Because of the incompatibility between VGCNF and polymer matrices, functionalization of VGCNF is an effective and required methodology to enhance the interaction between the nanofiller and polymer matrix. There is very little of literature on VGCNF/polymer composites prepared by in situ polymerization, coagulation, solution processing, grafted-VGCNF, and melt spinning. Studying the properties of VGCNF/polymer composite from these processes is essential in order to reveal the reinforcement effect of VGCNF and the ultimate properties that can be expected from their composites. Fortunately, much work has been done using CNTs and can be used as a guide for further development with VGCNFs.

Rheological properties of VGCNF/polymer composites showed that in most cases addition of VGCNF increases the complex viscosity and storage modulus. At high shear rate, viscosity of highly filled VGCNF/polymer composites is close to that of neat polymer because of the strong shear thinning behavior of the composites. Rheological percolation threshold was observed in some VGCNF/polymer composites. For VGCNF/PC composites, because of the poor adhesion between PC and VGCNF, VGCNF was found to act as ball-bearings that facilitate the movement of PC chains. Critical studies that need to be performed are studies comparing the rheological behavior of VGCNF/polymer composites to that of CNT/polymer composites, and studies on the rheological behavior of VGCNF/immiscible polymer blends. Since characterization of nanofiller aspect ratio is difficult and rheological properties of filled polymers are very sensitive to the filler dispersion and aspect ratio, the rheological properties might be used to estimate the dispersion and aspect ratio of nanofiller.

Depending on the polymer type, adding VGCNF could increase or decrease the level and the type of the host polymer's crystallinity, and thus affect the melting/crystallization temperature. The glass transition temperature was not affected for many polymers as a result of VGCNF addition. However, for epoxy and PMMA, an increase in T_g with increasing VGCNF content was found. The increase in T_g was due to the presence of nanofiber that restricted the segmental movements of polymer chains.

References

[1] Endo M, Kim YA, Hayashi T, Nishimura K, Matusita T, Miyashita K, et al. Vapor-grown carbon fibers (VGCFs) – basic properties and their battery applications. Carbon 2001;39(9):1287–97.

[2] Paul DR, Robeson LM. Polymer nanotechnology: nanocomposites. Polymer 2008;49(15):3187–204.

[3] Breuer O, Sundararaj U. Big returns from small fibers: a review of polymer/carbon nanotube composites. Polym Compos 2004;25(6):630–45.

[4] Maruyama B, Alam H. Carbon nanotubes and nanofibers in composite materials. SAMPE J 2002;38(3):59–70.

[5] Winey KI, Vaia RA. Polymer nanocomposites. MRS Bull 2007;32(4):314–9.

[6] Miyagawa H, Misra M, Mohanty AK. Mechanical properties of carbon nanotubes and their polymer nanocomposites. J Nanosci Nanotechnol 2005;5(10):1593–615.

[7] Mordkovich VZ. Carbon nanofibers: a new ultrahigh-strength material for chemical technology. Theor Found Chem Eng 2003;37(5):429–38.

[8] Tibbetts GG, Lake ML, Strong KL, Rice BP. A review of the fabrication and properties of vapor-grown carbon nanofiber/polymer composites. Compos Sci Technol 2007;67(7-8):1709–18.

[9] Harrats C, Groeninckx G. Features, questions and future challenges in layered silicates clay nanocomposites with semicrystalline polymer matrices. Macromol Rapid Commun 2008;29(1):14–26.

[10] Chen B, Evans JRG, Greenwell HC, Boulet P, Coveney PV, Bowden AA, et al. A critical appraisal of polymer–clay nanocomposites. Chem Soc Rev 2008;37(3):568–94.

[11] Pelsoci T. Composite manufacturing technologies: applications automotive, petroleum, and civil infrastructure industries; 2004.

[12] Al-Saleh MH, Sundararaj U. Effect of shear mixing conditions on EMI shielding effectiveness and electrical properties of VGCNF filled thermoplastic. In: Society of plastics engineers annual technical conference – ANTEC. Milwaukee, WI, USA; 2008. p. 34–8.

[13] Al-Saleh MH, Sundararaj U. A review of vapor grown carbon nanofiber/polymer conductive composites. Carbon 2009;47(1):2–22.

[14] Yang SY, Lozano K, Lomeli A, Foltz HD, Jones R. Electromagnetic interference shielding effectiveness of carbon nanofiber/LCP composites. Composites Part A 2005;36(5):691–7.

[15] Zhang B, Fu RW, Zhang MQ, Dong XM, Wang LC, Pittman CU. Gas sensitive vapor grown carbon nanofiber/polystyrene sensors. Mater Res Bull 2006;41(3):553–62.

[16] Subramanian V, Zhu HW, Wei BQ. High rate reversibility anode materials of lithium batteries from vapor-grown carbon nanofibers. J Phys Chem B 2006;110(14):7178–83.

[17] Zhou J-H, Chen C, Guo R, Fang X-C, Zhou X-G. Synthesis and characterization of carbon nanofiber/alumina composite by extrusion casting. Carbon 2009;47(8):2077–84.

[18] Shim BS, Starkovich J, Kotov N. Multilayer composites from vapor-grown carbon nano-fibers. Compos Sci Technol 2006;66(9):1174–81.

[19] Kim YA, Hayashi T, Fukai Y, Endo M, Yanagisawa T, Dresselhaus MS. Effect of ball milling on morphology of cup-stacked carbon nanotubes. Chem Phys Lett 2002;355(3–4):279–84.

[20] VanHattum FWJ, Serp P, Figueiredo JL, Bernardo CA. The effect of morphology on the properties of vapour-grown carbon fibres. Carbon 1997;35(6):860–3.

[21] Uchida T, Anderson DP, Minus ML, Kumar S. Morphology and modulus of vapor grown carbon nano fibers. J Mater Sci 2006;41(18):5851–6.

[22] Finegan IC, Tibbetts GG. Electrical conductivity of vapor-grown carbon fiber/thermoplastic composites. J Mater Res 2001;16(6):1668–74.

[23] Keith JM, Janda NB, King JA. Shielding effectiveness density theory for carbon fiber/nylon 6,6 composites. Polym Compos 2005;26(5):671–8.

[24] Coleman JN, Khan U, Gun'ko YK. Mechanical reinforcement of polymers using carbon nanotubes. Adv Mater 2006;18(6):689–706.

[25] Shaffer MSP, Windle AH. Fabrication and characterization of carbon nanotube/poly(vinyl alcohol) composites. Adv Mater 1999;11(11):937–41.

[26] Kim P, Shi L, Majumdar A, McEuen PL. Thermal transport measurements of individual multiwalled nanotubes. Phys Rev Lett 2001;87(21):215502.

[27] Xie XL, Mai YW, Zhou XP. Dispersion and alignment of carbon nanotubes in polymer matrix: a review. Mat Sci Eng R 2005;49(4):89–112.

[28] Al-Saleh MH, Sundararaj U. Processing–microstructure–property relationship in conductive polymer nanocomposites. Polymer 2010;51(12):2740–7.

[29] Jimenez GA, Jana SC. Electrically conductive polymer nanocomposites of polymethylmethacrylate and carbon nanofibers prepared by chaotic mixing. Composites Part A 2007;38(3):983–93.

[30] Miyagawa H, Rich MJ, Drzal LT. Thermo-physical properties of epoxy nanocomposites reinforced by carbon nanotubes and vapor grown carbon fibers. Thermochim Acta 2006;442(1–2):67–73.

[31] Thostenson ET, Li CY, Chou TW. Nanocomposites in context. Compos Sci Technol 2005;65(3–4):491–516.

[32] Merkulov VI, Lowndes DH, Wei YY, Eres G, Voelkl E. Patterned growth of individual and multiple vertically aligned carbon nanofibers. Appl Phys Lett 2000;76(24):3555–7.

[33] Endo M, Kim YA, Ezaka M, Osada K, Yanagisawa T, Hayashi T, et al. Selective and efficient impregnation of metal nanoparticles on cup-stacked-type carbon nanofibers. Nano Lett 2003;3(6):723–6.

[34] Endo M, Kim YA, Hayashi T, Fukai Y, Oshida K, Terrones M, et al. Structural characterization of cup-stacked-type nanofibers with an entirely hollow core. Appl Phys Lett 2002;80(7):1267–9.

[35] Coleman JN, Khan U, Blau WJ, Gun'ko YK. Small but strong: a review of the mechanical properties of carbon nanotube–polymer composites. Carbon 2006;44:1624–52.

[36] Tibbetts GG, Beetz CP. Mechanical properties of vapor grown carbon fibers. J Phys D: Appl Phys 1987;20(3):292–7.

[37] Patton RD, Pittman CU, Wang L, Hill JR. Vapor grown carbon fiber composites with epoxy and poly(phenylene sulfide) matrices. Composites Part A 1999;30(9):1081–91.

[38] Qian D, Wagner GJ, Liu WK, Yu MF, Ruoff RS. Mechanics of carbon nanotubes. Appl Mech Rev 2002;55(6):495–532.

[39] Krishnan A, Dujardin E, Ebbesen TW, Yianilos PN, Treacy MMJ. Young's modulus of single-walled nanotubes. Phys Rev B 1998;58(20):14013.

[40] Treacy MMJ, Ebbesen TW, Gibson JM. Exceptionally high Young's modulus observed for individual carbon nanotubes. Nature 1996;381(6584):678–80.

[41] Salvetat JP, Bonard JM, Thomson NB, Kulik AJ, Forró L, Benoit W, et al. Mechanical properties of carbon nanotubes. Appl Phys A: Mater Sci Process 1999;69(3):255–60.

[42] Salvetat JP, Briggs GAD, Bonard JM, Bacsa RR, Kulik AJ, Stöckli T, et al. Elastic and shear moduli of single-walled carbon nanotube ropes. Phys Rev Lett 1999;82(5):944–7.

[43] Salvetat JP, Kulik AJ, Bonard JM, Briggs GAD, Stockli T, Metenier K, et al. Elastic modulus of ordered and disordered multiwalled carbon nanotubes. Adv Mater 1999;11(2):161–5.

[44] Yu MF, Lourie O, Dyer MJ, Moloni K, Kelly TF, Ruoff RS. Strength and breaking mechanism of multiwalled carbon nanotubes under tensile load. Science 2000;287(5453):637–40.

[45] Xie S, Li W, Pan Z, Chang B, Sun L. Mechanical and physical properties on carbon nanotube. J Phys Chem Solids 2000;61(7):1153–8.

[46] Yang SY, Taha-Tijerina J, Serrato-Diaz V, Hernandez K, Lozano K. Dynamic mechanical and thermal analysis of aligned vapor grown carbon nanofiber reinforced polyethylene. Composites Part B 2007;38(2):228–35.

[47] Choi YK, Sugimoto K, Song SM, Gotoh Y, Ohkoshi Y, Endo M. Mechanical and physical properties of epoxy composites reinforced by vapor grown carbon nanofibers. Carbon 2005;43(10):2199–208.

[48] Bubert H, Haiber S, Brandl W, Marginean G, Heintze M, Bruser V. Characterization of the uppermost layer of plasma-treated carbon nanotubes. Diamond Relat Mater 2003;12(3–7):811–5.

[49] Schadler LS, Giannaris SC, Ajayan PM. Load transfer in carbon nanotube epoxy composites. Appl Phys Lett 1998;73(26):3842–4.

[50] Barrera EV. Key methods for developing single-wall nanotube composites. JOM 2000;52(11):A38–42.

[51] Tang BZ, Xu HY. Preparation, alignment, and optical properties of soluble poly(phenylacetylene)-wrapped carbon nanotubes. Macromolecules 1999;32(8):2569–76.

[52] Qian D, Dickey EC, Andrews R, Rantell T. Load transfer and deformation mechanisms in carbon nanotube–polystyrene composites. Appl Phys Lett 2000;76(20):2868–70.

[53] Biercuk MJ, Llaguno MC, Radosavljevic M, Hyun JK, Johnson AT, Fischer JE. Carbon nanotube composites for thermal management. Appl Phys Lett 2002;80(15):2767–9.

[54] Safadi B, Andrews R, Grulke EA. Multiwalled carbon nanotube polymer composites: synthesis and characterization of thin films. J Appl Polym Sci 2002;84(14):2660–9.
[55] Haggenmueller R, Gommans HH, Rinzler AG, Fischer JE, Winey KI. Aligned single-wall carbon nanotubes in composites by melt processing methods. Chem Phys Lett 2000;330(3–4):219–25.
[56] Ko F, Gogotsi Y, Ali A, Naguib N, Ye HH, Yang GL, et al. Electrospinning of continuous carbon nanotube-filled nanofiber yarns. Adv Mater 2003;15(14):1161–5.
[57] Park C, Ounaies Z, Watson KA, Crooks RE, Smith J, Lowther SE, et al. Dispersion of single wall carbon nanotubes by in situ polymerization under sonication. Chem Phys Lett 2002;364(3–4):303–8.
[58] Gong XY, Liu J, Baskaran S, Voise RD, Young JS. Surfactant-assisted processing of carbon nanotube/polymer composites. Chem Mater 2000;12(4):1049–52.
[59] Lin Y, Zhou B, Fernando KAS, Liu P, Allard LF, Sun YP. Polymeric carbon nanocomposites from carbon nanotubes functionalized with matrix polymer. Macromolecules 2003;36(19):7199–204.
[60] Hill DE, Lin Y, Rao AM, Allard LF, Sun YP. Functionalization of carbon nanotubes with polystyrene. Macromolecules 2002;35(25):9466–71.
[61] Kimura T, Ago H, Tobita M, Ohshima S, Kyotani M, Yumura M. Polymer composites of carbon nanotubes aligned by a magnetic field. Adv Mater 2002;14(19):1380–3.
[62] Lozano K, Bonilla-Rios J, Barrera EV. A study on nanofiber-reinforced thermoplastic composites (II): investigation of the mixing rheology and conduction properties. J Appl Polym Sci 2001;80(8):1162–72.
[63] Andrews R, Jacques D, Minot M, Rantell T. Fabrication of carbon multiwall nanotube/polymer composites by shear mixing. Macromol Mater Eng 2002;287(6):395–403.
[64] Al-Saleh MH, Sundararaj U. Electrically conductive carbon nanofiber/polyethylene composite: effect of melt mixing conditions. Polym Adv Technol 2010. doi:10.1002/pat.1526.
[65] Kumar S, Doshi H, Srinivasarao M, Park JO, Schiraldi DA. Fibers from polypropylene/nano carbon fiber composites. Polymer 2002;43(5):1701–3.
[66] Kuriger RJ, Alam MK, Anderson DP, Jacobsen RL. Processing and characterization of aligned vapor grown carbon fiber reinforced polypropylene. Composites Part A 2002;33(1):53–62.
[67] Jin ZX, Pramoda KP, Goh SH, Xu GQ. Poly(vinylidene fluoride)-assisted melt-blending of multi-walled carbon nanotube/poly(methyl methacrylate) composites. Mater Res Bull 2002;37(2):271–8.
[68] Tsubokawa N. Preparation and properties of polymer-grafted carbon nanotubes and nanofibers. Polym J 2005;37(9):637–55.
[69] Kearns JC, Shambaugh RL. Polypropylene fibers reinforced with carbon nanotubes. J Appl Polym Sci 2002;86(8):2079–84.
[70] Grady BP, Pompeo F, Shambaugh RL, Resasco DE. Nucleation of polypropylene crystallization by single-walled carbon nanotubes. J Phys Chem B 2002;106(23):5852–8.
[71] Lau KT, Hui D. Effectiveness of using carbon nanotubes as nano-reinforcements for advanced composite structures. Carbon 2002;40(9):1605–6.
[72] Potschke P, Fornes TD, Paul DR. Rheological behavior of multiwalled carbon nanotube/polycarbonate composites. Polymer 2002;43(11):3247–55.
[73] Ding W, Eitan A, Fisher FT, Chen X, Dikin DA, Andrews R, et al. Direct observation of polymer sheathing in carbon nanotube–polycarbonate composites. Nano Lett 2003;3(11):1593–7.
[74] Coleman JN, Cadek M, Ryan KP, Fonseca A, Nagy JB, Blau WJ, et al. Reinforcement of polymers with carbon nanotubes. The role of an ordered polymer interfacial region. Experiment and modeling. Polymer 2006;47(26):8556–61.
[75] Barber AH, Cohen SR, Wagner HD. Measurement of carbon nanotube–polymer interfacial strength. Appl Phys Lett 2003;82(23):4140–2.
[76] Frankland SJV, Caglar A, Brenner DW, Griebel M. Molecular simulation of the influence of chemical cross-links on the shear strength of carbon nanotube–polymer interfaces. J Phys Chem B 2002;106(12):3046.
[77] Cooper CA, Cohen SR, Barber AH, Wagner HD. Detachment of nanotubes from a polymer matrix. Appl Phys Lett 2002;81(20):3873–5.
[78] Tucker CL, Liang E. Stiffness predictions for unidirectional short-fiber composites: review and evaluation. Compos Sci Technol 1999;59(5):655–71.
[79] Weon JI, Sue HJ. Effects of clay orientation and aspect ratio on mechanical behavior of nylon-6 nanocomposite. Polymer 2005;46(17):6325–34.
[80] Cox HL. The elasticity and strength of paper and other fibrous materials. Brit J Appl Phys 1952;3:72–9.
[81] Shinichi S, Isao F, Yong C. Effects of fiber compression and length distribution on the flexural properties of short kenaf fiber-reinforced biodegradable composites. Polym Compos 2006;27(2):170–6.
[82] Carneiro OS, Covas JA, Bernardo CA, Caldeira G, Van Hattum FWJ, Ting JM, et al. Production and assessment of polycarbonate composites reinforced with vapour-grown carbon fibres. Compos Sci Technol 1998;58(3–4):401–7.
[83] Caldeira G, Maia JM, Carneiro OS, Covas JA, Bernardo CA. Production and characterization of innovative carbon fiber polycarbonate composites. Polym Compos 1998;19(2):147–51.
[84] Sandler J, Werner P, Shaffer MSP, Demchuk V, Altstadt V, Windle AH. Carbon–nanofibre-reinforced poly(ether ether ketone) composites. Composites Part A 2002;33(8):1033–9.
[85] Shui X, Chung DDL. Conducting polymer-matrix composites containing carbon filaments of submicron diameter. Int SAMPE Symp Exhib 1993:1869–75.
[86] Lozano K, Barrera EV. Nanofiber-reinforced thermoplastic composites. I. Thermoanalytical and mechanical analyses. J Appl Polym Sci 2001;79(1):125–33.
[87] Gordeyev SA, Ferreira JA, Bernardo CA, Ward LM. A promising conductive material: highly oriented polypropylene filled with short vapour-grown carbon fibres. Mater Lett 2001;51(1):32–6.
[88] Tibbetts GG, McHugh JJ. Mechanical properties of vapor-grown carbon fiber composites with thermoplastic matrices. J Mater Res 1999;14(7):2871–80.
[89] Maxwell B. Miniature injection molder minimizes residence time. SPE J 1972;28(2):24–7.
[90] Yang B, Sato M, Kuriyama T, Inoue T. Improvement of gram-scale mixer for polymer blending. J Appl Polym Sci 2006;99(1):1–5.
[91] Breuer O, Chen HB, Lin B, Sundararaj U. Simulation and visualization of flow in a new miniature mixer for multiphase polymer systems. J Appl Polym Sci 2005;97(1):136–42.
[92] Sundararaj U, Macosko CW, Nakayama A, Inoue T. Milligrams to kilograms – an evaluation of mixers for reactive polymer blending. Polym Eng Sci 1995;35(1):100–14.
[93] Maric M, Macosko CW. Improving polymer blend dispersions in mini-mixers. Polym Eng Sci 2001;41(1):118–30.
[94] Chung DDL. Carbon fiber composites. Elsevier; 1994.
[95] Brandl W, Marginean G, Chirila V, Warschewski W. Production and characterization of vapour grown carbon fiber/polypropylene composites. Carbon 2004;42(1):5–9.
[96] Chirila V, Marginean G, Iclanzan T, Merino C, Brandl W. Method for modifying mechanical properties of carbon nano-fiber polymeric composites. J Thermoplast Compos Mater 2007;20(3):277–89.
[97] Cortes P, Lozano K, Barrera EV, Bonilla-Rios J. Effects of nanofiber treatments on the properties of vapor-grown carbon fiber reinforced polymer composites. J Appl Polym Sci 2003;89(9):2527–34.
[98] Finegan IC, Tibbetts GG, Glasgow DG, Ting JM, Lake ML. Surface treatments for improving the mechanical properties of carbon nanofiber/thermoplastic composites. J Mater Sci 2003;38(16):3485–90.
[99] Ma HM, Zeng JJ, Realff ML, Kumar S, Schiraldi DA. Processing, structure, and properties of fibers from polyester/carbon nanofiber composites. Compos Sci Technol 2003;63(11):1617–28.
[100] Shofner ML, Lozano K, Rodriguez-Macias FJ, Barrera EV. Nanofiber-reinforced polymers prepared by fused deposition modeling. J Appl Polym Sci 2003;89(11):3081–90.
[101] Shofner ML, Rodriguez-Macias FJ, Vaidyanathan R, Barrera EV. Single wall nanotube and vapor grown carbon fiber reinforced polymers processed by extrusion freeform fabrication. Composites Part A 2003;34(11):1207–17.
[102] Zeng JJ, Saltysiak B, Johnson WS, Schiraldi DA, Kumar S. Processing and properties of poly(methyl methacrylate)/carbon nano fiber composites. Composites Part B 2004;35(2):173–8.
[103] Kuriger RJ, Alam MK. Extrusion conditions and properties of vapor grown carbon fiber reinforced polypropylene. Polym Compos 2001;22(5):604–12.
[104] Spitalsky Z, Tasis D, Papagelis K, Galiotis C. Carbon nanotube–polymer composites: chemistry, processing, mechanical and electrical properties. Prog Polym Sci 2010;35(3):357–401.
[105] Coleman JN, Cadek M, Blake R, Nicolosi V, Ryan KP, Belton C, et al. High-performance nanotube-reinforced plastics: understanding the mechanism of strength increase. Adv Funct Mater 2004;14(8):791–8.
[106] Liu TX, Phang IY, Shen L, Chow SY, Zhang WD. Morphology and mechanical properties of multiwalled carbon nanotubes reinforced nylon-6 composites. Macromolecules 2004;37(19):7214–22.
[107] Chang TE, Jensen LR, Kisliuk A, Pipes RB, Pyrz R, Sokolov AP. Microscopic mechanism of reinforcement in single-wall carbon nanotube/polypropylene nanocomposite. Polymer 2005;46(2):439–44.
[108] Velasco-Santos C, Martinez-Hernandez AL, Fisher FT, Ruoff R, Castano VM. Improvement of thermal and mechanical properties of carbon nanotube composites through chemical functionalization. Chem Mater 2003;15(23):4470–5.
[109] Mamedov AA, Kotov NA, Prato M, Guldi DM, Wicksted JP, Hirsch A. Molecular design of strong single-wall carbon nanotube/polyelectrolyte multilayer composites. Nat Mater 2002;1(3):190–4.
[110] Gao JB, Itkis ME, Yu AP, Bekyarova E, Zhao B, Haddon RC. Continuous spinning of a single-walled carbon nanotube-nylon composite fiber. J Am Chem Soc 2005;127(11):3847–54.
[111] Miyagawa H, Drzal LT. Effect of oxygen plasma treatment on mechanical properties of vapor grown carbon fiber nanocomposites. Composites Part A 2005;36(10):1440–8.
[112] Choi YK, Sugimoto KI, Song SM, Endo M. Mechanical and thermal properties of vapor-grown carbon nanofiber and polycarbonate composite sheets. Mater Lett 2005;59(27):3514–20.
[113] Du F, Scogna RC, Zhou W, Brand S, Fischer JE, Winey KI. Nanotube networks in polymer nanocomposites: rheology and electrical conductivity. Macromolecules 2004;37(24):9048–55.
[114] Pötschke P, Abdel-Goad M, Alig I, Dudkin S, Lellinger D. Rheological and dielectrical characterization of melt mixed polycarbonate-multiwalled carbon nanotube composites. Polymer 2004;45(26):8863–70.
[115] Hyun YH, Lim ST, Choi HJ, John MS. Rheology of poly(ethylene oxide)/organoclay nanocomposites. Macromolecules 2001;34(23):8084–93.
[116] Vermant J, Ceccia S, Dolgovskij MK, Maffettone PL, Macosko CW. Quantifying dispersion of layered nanocomposites via melt rheology. J Rheol 2007;51(3):429–50.

[117] Wagener R, Reisinger TJG. A rheological method to compare the degree of exfoliation of nanocomposites. Polymer 2003;44(24):7513–8.
[118] Wan T, Clifford MJ, Gao F, Bailey AS, Gregory DH, Somsunan R. Strain amplitude response and the microstructure of PA/clay nanocomposites. Polymer 2005;46(17):6429–36.
[119] Zhao J, Morgan AB, Harris JD. Rheological characterization of polystyrene–clay nanocomposites to compare the degree of exfoliation and dispersion. Polymer 2005;46(20):8641–60.
[120] Durmus A, Kasgoz A, Macosko CW. Linear low density polyethylene (LLDPE)/clay nanocomposites. Part I: structural characterization and quantifying clay dispersion by melt rheology. Polymer 2007;48(15):4492–502.
[121] Al-Saleh MH, Sundararaj U. Electrically conductive carbon nanofiber/polyethylene composite: effect of melt mixing conditions. Polym Adv Technol 2009;9999(9999):n/a.
[122] Kelarakis A, Yoon K, Somani RH, Chen X, Hsiao BS, Chu B. Rheological study of carbon nanofiber induced physical gelation in polyolefin nanocomposite melt. Polymer 2005;46(25):11591–9.
[123] Moniruzzaman M, Winey KI. Polymer nanocomposites containing carbon nanotubes. Macromolecules 2006;39(16):5194–205.
[124] Chambon F, Winter HH. Linear viscoelasticity at the gel point of a crosslinking PDMS with imbalanced stoichiometry. J Rheol 1987;31(8):683–97.
[125] Winter HH, Francois C. Analysis of linear viscoelasticity of a crosslinking polymer at the gel point. J Rheol 1986;30(2):367–82.
[126] Lozano K, Yang SY, Zeng Q. Rheological analysis of vapor-grown carbon nanofiber-reinforced polyethylene composites. J Appl Polym Sci 2004;93(1):155–62.
[127] Carneiro OS, Maia JM. Rheological behavior of (Short) carbon fiber/thermoplastic composites. Part 1: the influence of fiber type, processing conditions and level of incorporation. Polym Compos 2000;21(6):960–9.
[128] Lakdawala K, Salovey R. Rheology of polymers containing carbon black. Polym Eng Sci 1987;27(14):1035–42.
[129] Shenoy AV. Rheology of filled polymer systems. Springer-Verlag; 1999.
[130] Lin B, Sundararaj U, Potschke P. Melt mixing of polycarbonate with multi-walled carbon nanotubes in miniature mixers. Macromol Mater Eng 2006;291(3):227–38.
[131] Takahashi T, Yonetake K, Koyama K, Kikuchi T. Polycarbonate crystallization by vapor-grown carbon fiber with and without magnetic field. Macromol Rapid Commun 2003;24(13):763–7.
[132] Zhang C, Wu HF, Ma CA, Sumita M. Effect of vapor grown carbon fiber on non-isothermal crystallization kinetics of HDPE/PMMA blend. Mater Lett 2006;60(8):1054–8.
[133] Xu YJ, Higgins B, Brittain WJ. Bottom-up synthesis of PS-CNF nanocomposites. Polymer 2005;46(3):799–810.
[134] Dufresne A, Paillet M, Putaux JL, Canet R, Carmona F, Delhaes P, et al. Processing and characterization of carbon nanotube/poly(styrene-co-butyl acrylate) nanocomposites. J Mater Sci 2002;37(18):3915–23.
[135] Zhou YX, Pervin F, Jeelani S. Effect vapor grown carbon nanofiber on thermal and mechanical properties of epoxy. J Mater Sci 2007;42(17):7544–53.
[136] Green KJ, Dean DR, Vaidya UK, Nyairo E. Multiscale fiber reinforced composites based on a carbon nanofiber/epoxy nanophased polymer matrix: synthesis, mechanical, and thermomechanical behavior. Composites Part A 2009;40(9):1470–5.